Westinghouse Electric Corporation Energy Systems

Box 355
Pittsburgh Pennsylvania 15230-0355

NTD-NRC-96-4617
DCP/NRC0445
Docket No.: STN-52-003

January 4, 1996

Document Control Desk
U.S. Nuclear Regulatory Commission
Washington, D.C. 20555

ATTENTION: T. R. QUAY

SUBJECT: AP600 CONTAINMENT

Dear Mr. Quay:

Enclosed are two copies of information provided to address NRC open issues related to the AP600 steel containment. Included are a draft revision of Subsection 3.8.2 of the SSAR, a draft revision of Chapter 42 of the AP600 PRA, and responses to NRC requests for additional information.

The SSAR Subsection 3.8.2 includes changes in the text to address DSER open items and questions raised in meetings and on phone calls. The figures have also been updated. Once the revision of the sections is finalized, a number of figures will be deleted and unnecessary details removed from the remaining figures as shown in the draft figures. This action should resolve the question about proprietary information in this section. You may note that the information in this transmittal is nonproprietary.

The sections in Chapter 42 related to methodology have been updated to resolve open items. The results in Sections 42.5 and 42.6 have not been requantified pending NRC concurrence on the resolution of methodology open items.

The responses to the NRC requests for additional information are in response to a letter dated. September 14, 1995.

If you have any questions, please contact D. A. Lindgren at (412) 374-4856.

Brian A. McIntyre, Manager
Advanced Plant Safety and Licensing

/nja

Enclosures

cc: Diane Jackson, NRC
Nicholas J. Liparulo, Westinghouse (w/o Enclosures)

2645A

160016

E004.1/1

DRAFT

3.8 Design of Category I Structures

3.8.1 Concrete Containment

This subsection is not applicable to the AP600.

3.8.2 Steel Containment

3.8.2.1 Description of the Containment

3.8.2.1.1 General

This subsection describes the structural design of the steel containment vessel and its parts and appurtenances. The steel containment vessel is an integral part of the containment system whose function is described in Section 6.2. It serves both to limit releases in the event of an accident and to provide the safety related ultimate heat sink.

The containment vessel is an ASME metal containment. The information contained in this subsection is based on the design specification and preliminary design and analyses of the vessel. Final detailed analyses will be documented in the ASME Design Report.

The containment arrangement is indicated in the general arrangement figures in Section 1.2. The portion of the vessel above elevation 132′-3″ is surrounded by the shield building but is exposed to ambient conditions as part of the passive cooling flow path. A flexible watertight and airtight seal is provided at elevation 132′-3″ between the containment vessel and the shield building. The portion of the vessel below elevation 132′-3″ is fully enclosed within the shield building.

Figure 3.8.2-1 shows the containment vessel outline, including the plate configuration and crane girder. It is a freestanding, cylindrical steel vessel with ellipsoidal upper and lower heads. The containment vessel has the following design characteristics:

Diameter: 130 feet
Height: 189 feet 10 inches
Design code: ASME III, Div. 1
Material: SA537, Class 2
Design Pressure: 45 psig
Design Temperature: 280°F
Design External Pressure: 3.0 psid

The wall thickness in most of the cylinder and the heads is 1.625 inches. The wall thickness of the lowest course of the cylindrical shell is increased to 1.75 inches to provide margin in the event of corrosion in the embedment transition region. The heads are ellipsoidal with a major diameter of 130 feet and a height of 37 feet 7.5 inches.

DRAFT

The containment vessel includes the shell, hoop stiffeners and crane girder, equipment hatches, personnel airlocks, penetration assemblies, and miscellaneous appurtenances and attachments.

The polar crane is designed for handling the reactor vessel head during normal refueling. The crane girder and wheel assemblies are designed to support a special trolley to be installed in the event of steam generator replacement.

The containment vessel supports most of the containment air baffle as described in subsection 3.8.4. The air baffle is arranged to permit inspection of the exterior surface of the containment vessel. Steel plates are welded to the dome as part of the water distribution system, described in subsection 6.2.2. The polar crane system is described in subsection 9.1.5.

3.8.2.1.2 Containment Vessel Support

The bottom head is embedded in concrete, with concrete up to elevation 100′ on the outside and approximately elevation 108′ on the inside. The containment vessel is assumed as an independent, free-standing structure above elevation 100′ The thickness of the lower head is the same as that of the upper head. There is no reduction in shell thickness even though credit could be taken for the concrete encasement of the lower head.

Vertical and lateral loads on the containment vessel and internal structures are transferred to the basemat below the vessel by friction and bearing. Seals are provided at the top of the concrete on the inside and outside of the vessel to prevent moisture between the vessel and concrete. A typical cross section design of the seal is presented in Figure 3.8.2-8, sheets 1 and 2. Furthermore, the concrete floor area and curb inside containment near Elevation 108' and the concrete slab outside containment at Elevation 100' slope away from the steel containment vessel to preclude water ponding adjacent to the vessel.

3.8.2.1.3 Equipment Hatches

Two equipment hatches are provided. One is at the operating floor (el. 135′-3″). The hatch has an inside diameter of 22 feet sized to permit replacement of a steam generator. The other is at floor elevation 107′-2″ to permit grade-level access into the containment with an inside diameter of 16 feet. The hatches, shown in Figure 3.8.2-2, consist of a cylindrical sleeve with a pressure seated dished head bolted on the inside of the vessel. The containment internal pressure acts on the convex face of the dished head and the head is in compression. The flanged joint has double O-ring or gum-drop seals with an annular space that may be pressurized for leak testing the seals.

3.8.2.1.4 Personnel Airlocks

Two personnel airlocks are provided, one located adjacent to each of the equipment hatches. Figure 3.8.2-3 shows the typical arrangement. Each personnel airlock has about a 10 foot external diameter to accommodate a door opening of width 3 feet, 6 inches and height 6 feet, 8 inches. The airlocks are long enough to provide a clear distance of eight feet which is not

impaired by the swing of the doors within the lock. The airlocks extend radially out from the containment vessel through the shield building. They are supported by the containment vessel.

Each airlock has two double-gasketed, pressure-seated doors in series. The doors are mechanically interlocked to prevent simultaneous opening of both doors and to allow one door to be completely closed before the second door can be opened. The interlock can be bypassed by using special tools and procedures.

3.8.2.1.5 Mechanical Penetrations

The mechanical penetrations consist of the fuel transfer penetration and mechanical piping penetrations and are listed in Table 6.2.3-4.

Figure 3.8.2-4, sheet 1, shows typical details for the mainsteam penetration. This includes bellows to minimize piping loads applied to the containment vessel and a guardpipe to protect the bellows and to prevent overpressurization of the containment annulus in a postulated pipe rupture event. Similar details are used for the feedwater penetration.

Figure 3.8.2-4, sheet 2, shows typical details for the startup feedwater penetration. This includes a guardpipe to prevent overpressurization of the containment annulus in a postulated pipe rupture event. Similar details are used for the steam generator blowdown penetration.

Figure 3.8.2-4, sheet 3, shows typical details for the normal residual heat removal penetration. Similar details are used for other penetrations below elevation 107′ 2″ where there is concrete inside the containment vessel. The flued head is integral with the process piping and is welded to the containment sleeve. The welds are accessible for inservice inspection. The containment sleeve is separated from the concrete by compressible material.

Figure 3.8.2-4, sheet 4 shows typical details for the other mechanical penetrations. These consist of a sleeve welded to containment with either a flued head welded to the sleeve (detail A), or with the process piping welded directly to the sleeve (detail B). Flued heads are used for stainless piping greater than 2 inches in nominal diameter and for piping with high operating temperatures.

Design requirements for the mechanical penetrations are as follows:

- Design and construction of the process piping follow ASME, Section III, Subsection NC. Design and construction of the remaining portions follow ASME Code, Section III, Subsection NE. The boundary of jurisdiction is according to ASME Code, Section III, Subsection NE.

- Penetrations are designed to maintain containment integrity under design basis accident conditions, including pressure, temperature and radiation.

- Guard pipes are designed for pipe ruptures as described in subsection 3.6.2.1.1.4.

- Bellows are stainless steel or nickel alloy and are designed to accommodate axial and lateral displacements between the piping and the containment vessel. These displacements include thermal growth of the mainsteam and feedwater piping during plant operation, relative seismic movements, and containment accident and testing conditions. Cover plates are provided to protect the bellows from foreign objects during construction and operation. These cover plates are removable to permit in-service inspection.

The fuel transfer penetration, shown in Figure 3.8.2-4, sheet 5, is provided to transfer fuel between the containment and the fuel handling area of the auxiliary building. The fuel transfer tube is welded to the penetration sleeve. The containment boundary is a double-gasketed blind flange at the refueling canal end. The expansion bellows are not a part of the containment boundary. Rather, they are water seals during refueling operations and accommodate differential movement between the containment vessel, containment interior structures, and the auxiliary building.

3.8.2.1.6 Electrical Penetrations

Figure 3.8.2-4, sheet 6, shows a typical 12 inch diameter electrical penetrations. The penetration assemblies consist of three (or six modules in a similar 18 inch diameter penetration) passing through a bulkhead attached to the containment nozzle. Electrical design of these penetrations is described in subsection 8.3.1.1.5.

Electrical penetrations are designed to maintain containment integrity under design basis accident conditions, including pressure, temperature, and radiation. Double barriers permit testing of each assembly to verify that containment integrity is maintained. Design and test is according to IEEE Standard 317-83 and IEEE Standard 323-83.

3.8.2.2 Applicable Codes, Standards, and Specifications

The containment vessel is designed and constructed according to the 1992 edition of the ASME Code, Section III, Subsection NE, Metal Containment. The Combined License applicant may update the Code edition and addenda as defined in subsection 5.2.1.1.

Structural steel nonpressure parts, such as ladders, walkways, and handrails are designed to the requirements for steel structures defined in subsection 3.8.4.

Section 1.9 discusses compliance with the Regulatory Guides and the Standard Review Plans.

3.8.2.3 Loads and Load Combinations

Table 3.8.2-1 summarizes the design loads, load combinations and ASME Service Levels. They meet the requirements of the ASME Code, Section III, Subsection NE. The containment vessel is designed for the following loads specified during construction, test, normal plant operation and shutdown, and during accident conditions:

DRAFT

D Dead loads or their related internal moments and forces, including any permanent piping and equipment loads.

L Live loads or their related internal moments and forces, including crane loads.

P_o Operating pressure loads during normal operating conditions resulting from pressure variations either inside or outside containment.

T_o Thermal effects and loads during normal operating conditions, based on the most critical transient or steady-state condition.

R_o Pipe reactions during normal operating conditions, based on the most critical transient or steady-state condition.

W Loads generated by the design wind on the portion of the containment vessel above elevation 132′, as described in subsection 3.3.1.1.

E_s Loads generated by the safe shutdown earthquake (SSE) as described in Section 3.7.

W_t Loads generated by the design tornado on the portion of the containment vessel above elevation 132′ as described in subsection 3.3.2.

P_t Test pressure.

P_d Containment vessel design pressure that exceeds the pressure load generated by the postulated pipebreak accidents and passive cooling function.

P_e Containment vessel external pressure

T_a Thermal loads under thermal conditions generated by the postulated break or passive cooling function and including T_o. This includes variations around the shell due to the surrounding buildings and maldistribution of the passive containment cooling system water.

R_a Pipe reactions under thermal conditions generated by the postulated break, as described in Section 3.6, and including R_o.

Y_r Loads generated by the reaction on the broken high-energy pipe during the postulated break, as described in Section 3.6.

Y_j Jet impingement load on a structure generated by the postulated break, as described in Section 3.6.

Y_m Missile impact load on a structure generated by or during the postulated break, as from pipe whipping, as described in Section 3.6.

Note that loads associated with flooding of the containment below elevation 107′ are resisted by the concrete structures and not by the containment vessel.

3.8.2.4 Design and Analysis Procedures

The design and analysis procedures for the containment vessel are according to the requirements of the ASME Code, Section III, Subsection NE.

The analyses are summarized in Table 3.8.2-4. The detailed analyses will use a series of general-purpose finite element, axisymmetric shell and special purpose computer codes to conduct such analyses. Code development, verification, validation, configuration control and error reporting and resolution are according to the Quality Assurance requirements of Chapter 17.

3.8.2.4.1 Analyses for Design Conditions

3.8.2.4.1.1 Axisymmetric Shell Analyses

The containment vessel is modelled as an axisymmetric shell and analyzed using general shell of revolution computer programs. A model used for static analyses is shown in Figure 3.8.2-~~76~~. The programs calculate displacements and stresses in thin walled, elastic, shells of revolution when subjected to edge, surface, and/or temperature loads with arbitrary distribution over the surface of the shell. Three different types of analyses are available in these computer programs:

1) Static analysis can be performed for any arbitrary loading distribution. Longitudinally, concentrated loads may be applied at panel ends and distributed loads may be applied varying between specified points within each panel. The circumferential distribution is obtained through the use of Fourier Series.

2) Natural frequencies, mode shapes (displacements and forces), and participation factors for any loading that can be handled statically can be calculated and output to a file for use in either a spectral analysis, when a response spectrum is available, or in a modal superposition analysis, when transient forcing functions of the form $g(s,\theta).f(t)$ are available. The program can handle extra concentrated and distributed mass acting in any or all directions plus fluid structure interaction.

3) Direct time integration analysis for general transient problems can be calculated where the forcing function cannot readily be separated into separate spatial and temporal functions. As in natural frequency analysis, additional concentrated and distributed masses acting in any and all directions can be applied. Pressures can vary in an arbitrary fashion versus time and damping may be included.

Dynamic analyses of the axisymmetric model, which is similar to that shown in Figure 3.8.2-6, are performed to obtain frequencies and mode shapes. These are used to confirm the adequacy of the containment vessel stick model as described in subsection 3.7.2.3.2. Static stress analyses are performed for each of the following loads.

- Dead load
- Internal pressure
- Equivalent static seismic accelerations
- Polar crane wheel loads
- Wind loads
- Thermal loads

The equivalent static accelerations applied in the seismic analysis are the maximum acceleration responses based on the envelope of the results for each soil case. These accelerations are applied as separate load cases in the east-west, north-south and vertical directions. The torsional moments, which include the effects of the eccentric masses, are increased to account for accidental torsion and are evaluated in a separate calculation.

The results of these load cases are factored and combined in accordance with the load combinations identified in Table 3.8.2-1. These results are used to evaluate the general shell away from local penetrations and attachments, i.e. for areas of the shell represented by the axisymmetric geometry. The results for the polar crane wheel loads are also used to establish local shell stiffnesses for inclusion in the containment vessel stick model described in subsection 3.7.2.3. The results of the analyses and evaluations are included in the containment vessel design report.

Design of the containment shell is primarily controlled by the internal pressure of 45 psig. The meridional and circumferential stresses for the internal pressure case are shown in Figure 3.8.2-5. The most highly stressed regions for this load case are the portions of the shell away from the hoop stiffeners and the knuckle region of the top head. In these regions the stress intensity is close to the allowable for the design condition.

Major loads that induce compressive stresses in the containment vessel are internal and external pressure and crane and seismic loads. Each of these loads and the evaluation of the compressive stresses are discussed below.

- Internal pressure causes compressive stresses in the knuckle region of the top head and in the equipment hatch covers. The evaluation methods are similar to those discussed in subsection 3.8.2.4.2 for the ultimate capacity.

- Evaluation of external pressure loads is performed in accordance with ASME Code, Section III, Subsection NE, Paragraph NE-3133.

- Crane wheel loads due to crane dead load, live load, and seismic loads result in local compressive stresses in the vicinity of the crane girder. These are evaluated in accordance with ASME Code Case N-284, Revision 1.

- Overall seismic loads result in axial compression and tangential shear stresses at the base of the cylindrical portion. These are evaluated in accordance with ASME Code Case N-284, Revision 1.

The bottom head is embedded in the concrete base at elevation 100 feet. This leads to circumferential compressive stresses at the discontinuity under thermal loading associated with the design basis accident. The containment vessel design includes a Service Level A combination in which the vessel above elevation 100′ is conservatively specified at the design temperature of 280°F and the portion of the embedded vessel (and concrete) is specified at a temperature of 70°F. Containment shell buckling close to the base is evaluated against the criteria of ASME Code Case N-284, Revision 1, using a BOSOR-5 model of the portion of the shell above elevation 100′ extending up to the horizontal stiffener at elevation 132′ 3″. Material yield and stiffness properties are based on properties at the design temperature of 280°F. Temperature differences are raised by small increments until buckling is predicted. Buckling occurred 20 inches above elevation 100′ for a circumferential wave number, N = 190, at a factor of 6.0 times the design differential temperature condition. The half buckling wave length is less than 0.5 $\sqrt{(rt)}$. This is not a significant buckling issue; buckling did not occur for wave numbers below N = 60, which is the critical range for the cylinder and top head under external and internal pressure.

3.8.2.4.1.2 Local Analyses

The penetrations and penetration reinforcements are designed in accordance with the rules of ASME III, Subsection NE. The dynamic response of the local concentrated mass is considered in local analyses of the shell and is included in the design.

Finite element analyses are performed to confirm that the design of the penetration in accordance with the ASME code results in acceptable buckling safety factors. A finite element ANSYS model, as shown in Figure 3.8.2-7, represents the portion of the vessel close to the embedment with the lower equipment hatch and personnel airlock. This is analyzed for external pressure and axial loads and demonstrates that the penetration reinforcement is sufficient and that the lowest buckling mode occurs in the shell away from the penetrations and embedment.

3.8.2.4.2 Evaluation of Ultimate Capacity

The capacity of the containment vessel has been calculated for internal pressure loads for use in the probabilistic risk assessment analyses and severe accident evaluations. Each element of the containment vessel boundary was evaluated to estimate the maximum pressure at an ambient temperature of 100°F corresponding to the following stress and buckling criteria:

- Deterministic severe accident pressure capacity corresponding to ASME Service Level C limits on stress intensity, Code Case N-284 for buckling of the equipment hatch covers, and sixty percent of critical buckling for the top head. The deterministic severe accident pressure capacity corresponds to the approach in SECY 93-087, to maintain a reliable

leak-tight barrier approximately 24 hours following the onset of core damage under the more likely severe accident challenges. This approach was approved by the Nuclear Regulatory Commission as outline in the Staff Requirements Memorandum on SECY-93-087 - Policy, Technical, and Licensing Issues Pertaining to Evolutionary and Advanced Light Water Reactor (ALWR) Designs, Dated July 21, 1993.

- Best estimate capacity corresponding to gross membrane yield at the ASME-specified minimum yield stress (SA537, Class 2, yield stress = 60 ksi, ultimate stress = 80 ksi), and critical buckling for the equipment hatch covers and top head.

The results are shown in Table 3.8.2-2. The analyses at a temperature of 100°F are described in the following paragraphs for each element. The critical regions identified in this table are then examined further for their response at higher temperature. This results in the best-estimate capacity based on the ASME-specified minimum yield properties. The evaluation considered the containment boundary elements including:

- Cylindrical shell
- Top and bottom heads
- Equipment hatches and covers
- Personnel airlocks
- Mechanical and electrical penetrations

The evaluation identified the most likely failure mode to be that associated with gross yield of the cylindrical shell. Loss of containment function would be expected to occur because the large post-yield deflections would lead to local failures at penetrations, bellows, or other local discontinuities.

3.8.2.4.2.1 Tensile Stress Evaluation of Shell

Results of the axisymmetric analyses of the cylinder and top head described in subsection 3.8.2.4.1 for dead load and internal pressure were evaluated to determine the pressure at which stresses reach yield at ambient temperature of 100°F. The analyses assume the shell is fixed at elevation 100′, where the bottom head is embedded in concrete. The steel bottom head is identical to the top head and has a pressure capability greater than the top head due to the additional strength of the embedment concrete.

The allowable stress intensity under Service Level C loads is equal to yield. This corresponds to an internal pressure of 125 psig. The critical section is the cylinder, where the general primary membrane stress intensity is greatest.

The best-estimate yield analysis uses the von Mises criterion to establish yield rather than the more conservative ASME stress intensity approach. This increases the yield stress by about 15 percent for the cylinder, where the longitudinal stress is equal to one-half of the hoop stress resulting in first yield at an internal pressure of 144 psig. At this pressure, hoop stresses in the cylinder reach yield. The radial deflection is about 1.6 inches. As pressure increases further, large deflections occur. For a material such as SA537, where the yield plateau extends

from a strain of 0.2% to 0.6%, deflections would increase to 4.8 inches at yield without a substantial increase in pressure. Strain hardening would then permit a further increase in pressure with large radial deflections, as described in subsection 3.8.2.4.2.6.

3.8.2.4.2.2 Buckling Evaluation of Top Head

The top head has a radius-to-height ratio of 1.728. This is not as shallow as most ellipsoidal or torispherical heads, which typically have a radius-to-height ratio of 2. The ratio was specifically selected to minimize the local stresses and buckling in the knuckle region due to internal pressure. As the ratio decreases, the magnitude of compressive stresses in the knuckle region decreases; for a radius-to-height ratio of 1.4 or smaller, there are no compressive stresses and therefore there is no potential for buckling.

Theoretical Buckling Capacity

The top head was analyzed using the BOSOR-5 computer code (Reference 1). This code permits consideration of both large displacements and nonlinear material properties. It calculates shell stresses and checks stability at each load step. Yield of the cylinder started at a pressure of 144 psig using elastic - perfectly plastic material properties, a yield stress of 60 ksi, and the von Mises yield criterion. Yield of the top of the crown started at an internal pressure of 146 psig. Yield of the knuckle region started at 152 psig. A theoretical plastic buckling pressure of 174 psig was determined. At this pressure, the maximum effective prebuckling strain was 0.23 percent in the knuckle region where buckling occurred and 2.5 percent at the crown. The maximum deflection at the crown was 15.9 inches. A similar analysis was performed using non-linear material properties considering the effects of residual stresses; buckling did not occur in this analysis, and failure would occur once strains at the crown reach ultimate.

Predicted Pressure Capacity

The actual buckling capacity may be lower than the theoretical buckling capacity because of effects not included in the analysis such as imperfections and residual stresses. This is considered by the use of capacity reduction factors that are based upon a correlation of theory and experiment. The capacity reduction factor for the top head was evaluated based on comparisons of BOSOR-5 analyses against test results of ellipsoidal and torispherical heads. This evaluation is described below and concludes that no reduction in capacity need be considered; i.e. a capacity reduction factor of 1.0 is appropriate.

The knuckle region of ellipsoidal and torispherical heads is subjected to meridional tension and circumferential compression. The meridional tension tends to stabilize the knuckle region and reduces its sensitivity to imperfection. The radius-to-height ratio of 1.728 of the AP600 head results in a larger ratio of meridional tension to circumferential compression than on shallower heads, further reducing the sensitivity to imperfection.

Welding Research Council Bulletin 267 (Reference 22) shows a comparison of BOSOR-5 predictions of buckling against the results of 20 tests of small head models. These results are summarized in Table 4 of the reference and show ratios (capacity reduction factors) of actual buckling to the BOSOR-5 prediction with an average of 1.2. Only one of the 20 cases shows a capacity reduction factor less than 1.0.

Table 3.8.2-3 shows the key parameters, test results, and BOSOR-5 predictions for two large, fabricated 2:1 torispherical heads tested and reported in NUREG/CR-4926 (Reference 23). The theoretical plastic buckling pressure predicted by BOSOR-5 represents initial buckling based on actual material properties. The initial buckling did not cause failure for either of the tests, and test pressure continued to increase until rupture occurred in the spherical cap. The collapse pressures were three to four times the initial buckling pressures.

- **Test Head 1** - The test result of 58 psig is 79 percent of the predicted theoretical plastic buckling pressure of 74 psig. Many of the buckles occurred directly on the meridional weld seams of the knuckle. The knuckle welds were noticeably flatter than the corresponding welds of the Test 2 head. The as-built configuration extended inside the theoretical shape at some of the meridional weld seams and was most pronounced at the location of the first observed buckle. Model 1 exceeded the tolerances for formed heads specified for containment vessels in NE-4222.2 of ASME Section III, Subsection NE.

- **Test Head 2** - The test result of 106 psi is 100 percent of the BOSOR-5 predicted theoretical plastic buckling pressure. For test head 2, the welds had no noticeable flat spots and there was a smooth transition between the sphere and knuckle sections. Test head 2 was well within the Code allowable deviations.

The low-capacity reduction factor of 0.79 for test head 1 is attributed to excessive imperfections associated with the fabrication of relatively thin plate (0.196 inch). These imperfections were visible and were outside the tolerances permitted by the ASME Code. The results of test head 1 are therefore not considered applicable to the AP600. The results of test head 2 and of the small-scale models described in the Welding Research Council Bulletin support the application of a capacity reduction factor of 1.0.

The capacity of the AP600 head was also investigated using an approach similar to that permitted in ASME Code Case N284. This code case provides alternate rules for certain containment vessel geometries such as cylindrical shells. The theoretical elastic buckling pressure was calculated to be 536 psi using the linear elastic computer code, BOSOR-4 (Reference 24). A reduction factor (defined as the product of the capacity reduction factor and the plastic reduction factor) was established as 0.385 based on the lower bound curve of test results of 20 ellipsoidal and 28 torispherical tests specimens, which also include the two large fabricated heads previously discussed. This resulted in a predicted buckling capacity of 206 psig.

The preceding paragraphs addressed incipient buckling. It is concluded that buckling would not occur prior to reaching the pressure of 174 psig predicted in the BOSOR-5 analyses. Tests indicate that pressure can be significantly increased prior to rupture after the formation of the

initial buckles. - The best estimate capacity of the head is taken as the theoretical plastic buckling pressure of 174 psig predicted in the BOSOR-5 analyses

The Deterministic severe accident pressure capacity is taken as sixty percent of critical buckling. This is consistent with the safety factor for Service Level C in ASME Code Case N-284 and results in a containment head capacity of 104 psig.

3.8.2.4.2.3 Equipment Hatches

The equipment hatch covers were evaluated for buckling according to ASME Code Case N-284. The containment internal pressure acts on the convex face of the dished head and the hatch covers are in compression under containment internal pressure loads. The critical buckling capacity is based on classical buckling capacities reduced by capacity reduction factors to account for the effects of imperfections and plasticity. These capacity reduction factors are based on test data and are generally lower-bound values for the tolerances specified in the ASME code.

The critical buckling pressures are 195 psig for the 22 foot diameter hatch and 160 psig for the 16 foot diameter hatch at ambient temperature of 100°F. For the Service Level C limits a safety factor of 1.67 is specified, resulting in capabilities of 117 psig (22' dia) and 96 psig (16' dia).

Typical gaskets have been tested for severe accident conditions as described in NUREG/CR-5096 (Reference 25). The gaskets for the AP600 will be similar to those tested with material such as Presray EPDM E 603. For such gaskets the onset of leakage occurred at a temperature of about 600°F.

3.8.2.4.2.4 Personnel Airlocks

The capacity of the personnel airlocks was determined by comparing the airlock design to that tested and reported in NUREG/CR-5118 (Reference 3). Critical parameters are the same, so the results of the test apply directly. In the tests the inner door and end bulkhead of the airlock withstood a maximum pressure of 300 psig at 400°F. The capacity of the airlock is therefore at least 300 psig at ambient temperature. The maximum pressure corresponding to Service Level C is conservatively estimated by reducing this capacity in the ratio of the minimum specified material yield to ultimate.

3.8.2.4.2.5 Mechanical and Electrical Penetrations

Subsections 3.8.2.1.3 through 3.8.2.1.6 describe the containment penetrations. Penetration reinforcement is designed following the area replacement method of the ASME Code. The insert plates and sleeves permit development of the hoop tensile yield stresses predicted as the limiting capacity in subsection 3.8.2.4.1. Capacities of the equipment hatch covers are discussed in subsection 3.8.2.4.2.3 and of the personnel airlocks in subsection 3.8.2.4.2.4.

Mechanical penetrations welded directly to the containment vessel are generally piping systems with design pressures greater than that of the containment vessel. Thicknesses of the flued head or end plate are established based on piping support loads or stiffness requirements. The capacities of these penetrations are greater than the capacity of the containment vessel cylinder.

Mechanical penetrations for the large-diameter high-energy lines, such as the main steam and feedwater piping, include expansion bellows. The piping and flued head have large pressure capability. The response of expansion bellows to severe pressure and deformations is described in NUREG/CR-5561 (Reference 4). The bellows can withstand large pressure loading but may tear once the containment vessel deflection becomes large. Testing reported in NUREG/CR-6154 (Reference 26) has shown that the bellows remain leaktight even when subjected to large deflections sufficient to fully compress the bellows. Such large deflections do not occur so long as the containment vessel remains elastic. As described in subsection 3.8.2.4.2.6, the radial deflection of the shell increases substantially once the containment cylinder yields. The resulting deflections are assumed to cause loss of containment function. The containment penetration bellows are designed for a pressure of 90 psig at design temperature within Service Level C limits, concurrent with the relative displacements imposed on the bellows when the containment vessel is pressurized to these magnitudes.

Electrical penetrations have a pressure boundary consisting of the sleeve and an end plate containing a series of modules. The pressure capacity of these elements is large and is greater than the capacity of the containment vessel cylinder at temperatures up to the containment design temperature. Electrical penetration assemblies are also designed to satisfy ASME Service Level C stress limits under a pressure of 90 psig at design temperature. Tests at pressures and temperatures representative of severe accident conditions are described in NUREG/CR-5334 (Reference 5), where the Westinghouse penetrations were irradiated, aged, then tested to 75 psia at 400°F. Other electrical penetration assemblies were tested to higher pressures and temperatures. These tests showed that the electrical penetration assemblies withstand severe accident conditions. The electrical penetration assemblies are qualified for the containment design basis event conditions as described in Appendix 3D. The assemblies are similar to one of those tested by Sandia as reported in NUREG/CR-5334 (Reference 5). The ultimate pressure capacity of the electrical penetration assemblies is primarily determined by the temperature. The maximum temperature of the containment vessel below the operating deck during a severe accident is approximately equal to the containment design temperature of 280°F. This temperature is significantly below the temperature at which the assemblies from the three suppliers in the Sandia tests were tested.

3.8.2.4.2.6 Material Properties

The containment vessel is designed using SA537, Class 2 material. This has a specified minimum yield of 60 ksi and ultimate of 80 ksi. Test data for materials meeting SA537 or having similar chemical properties were reviewed. In a sample of 122 tests for thicknesses equaling or exceeding 1.50 inches and less than 1.75 inches, the actual yield had a mean value of 69.1 ksi with a standard deviation of 3.3 ksi. Thus, the actual yield is expected to be about

DRAFT

15 percent higher than the minimum yield. Membrane yield of the cylinder is predicted to occur at an internal pressure of 166 psig.

A stress-strain curve for material with chemistry similar to SA537, Class 2, indicated constant yield stress of 81.3 ksi from a strain of 0.002 to 0.006 followed by strain-hardening up to a maximum stress of 94.5 ksi at a strain of 0.079. The first portion of the strain-hardening is nearly linear, with a stress of 90 ksi at a strain of 4 percent. This strain occurs at a stress 10 percent above yield. Thus, a pressure load 10 percent higher than that corresponding to yield of the shell would result in 4 percent strain and a 31 inch radial deflection of the containment cylinder. Such a deflection is expected to cause major distress for penetrations, the air flow path, and local areas where other structures are close to the containment vessel. Loss of function is therefore assumed for the containment once gross yield of the containment cylinder occurs.

3.8.2.4.2.7 Effect of Temperature

The evaluations described in the preceding subsections are based on an ambient temperature of 100°F. Nonmetallic items, such as gaskets, are qualified to function at the design temperature. The capacity of steel elements is reduced in proportion to the reduction due to temperature in yield stress, ultimate stress, or elastic modulus. The cylinder is governed by yield stress, and elastic buckling of the hatch covers is governed by the elastic modulus. The reduction in capacity is estimated using the tables given for material properties in the ASME Code. At 400°F, the yield stress is reduced by 17 percent and the pressure capacity corresponding to gross yield is reduced from 144 to 120 psig.

3.8.2.4.2.8 Summary of Containment Pressure Capacity

The ultimate pressure capacity for containment function is expected to be associated with leakage caused by excessive radial deflection of the containment cylindrical shell. This radial deflection causes distress to the mechanical penetrations, and leakage would be expected at the expansion bellows for the main steam and feedwater piping. There is high confidence that this failure would not occur before stresses in the shell reach the minimum specified material yield. This is calculated to occur at a pressure of 144 psig at ambient temperature and 120 psig at 400°F. Failure would be more likely to occur at a pressure about 15 percent higher based on expected actual material properties.

The deterministic severe accident pressure that can be accommodated according to the ASME Service Level C stress intensity limits and using a factor of safety of 1.67 for buckling of the top head is determined by the capacity of the 16 foot diameter equipment hatch cover and the ellipsoidal head. The maximum capacity of the hatch cover, calculated according to ASME Code Case N-284 Service Level C, is 96 psig at ambient temperature of 100°F and 93 psig at 280°F. The maximum capacity of the ellipsoidal head is 104 psig at 100°F and 92 psig at 280°F.

Draft

3.8.2.5 Structural Criteria

The containment vessel is designed, fabricated, installed, and tested according to the ASME Code, Section III, Subsection NE, and will receive a code stamp.

Stress intensity limits are according to ASME Code, Section III, Paragraph NE-3221 and Table NE-3221-1. Critical buckling stresses are checked according to the provisions of ASME Code, Section III, Paragraph NE-3222, or ASME Code Case N-284.

3.8.2.6 Materials, Quality Control, and Special Construction Techniques

Materials for the containment vessel, including the equipment hatches, personnel locks, penetrations, attachments, and appurtenances meet the requirements of NE-2000 of the ASME Code. The basic containment material is SA537, Class 2, plate. This material has been selected to satisfy the lowest service metal temperature requirement. This temperature is established for the portion of the vessel exposed to the environment as the minimum ambient air temperature which is site specific. Temperatures as low as -40°F (see Table 2.0-1) are acceptable for SA537, Class 2 material. Impact test requirements are as specified in NE-2000.

The containment vessel is coated with an inorganic zinc coating, except for those portions fully embedded in concrete. The inside of the vessel below the operating floor and up to eight feet above the operating floor also has a phenolic top coat. Below elevation 100′ the vessel is fully embedded in concrete with the exception of the few penetrations at low elevations (see Figure 3.8.2-4, sheet 3 of 6 for typical details). Embedding the steel vessel in concrete protects the steel from corrosion.

The AP600 configuration is shown in the general arrangement figures in Section 1.2 and in Figure 3.8.2-1. The exterior of the vessel is embedded at elevation 100′ and concrete is placed against the inside of the vessel up to elevation 108′-2″. Above this elevation the inside and outside of the containment vessel are accessible for inspection of the coating. The vessel is coated with an inorganic zinc primer to a level just below the concrete. Seals are provided at the surface of the concrete inside and outside the vessel so that moisture is not trapped next to the steel vessel just below the top of concrete. The seal on the inside accommodates radial growth of the vessel due to pressurization and heatup.

The plate thickness for the first course (elevation 104′1.5″ to 116′10″) of the cylinder is 1.75 inches, which is one eighth of an inch thicker than the rest of the vessel. This provides margin in the event that there would be any corrosion in the transition region despite the coatings and seals described above. Equivalent margin is available for the 1.625 inch thick bottom head in the transition region (elevation 100′-104′1.5″). The plate thickness for the head is a constant thickness and is established by the stresses in the knuckle. As a result, the pressure stresses in the transition zone are well below the allowable stress providing margin in the event of corrosion in this region.

The quality control program involving welding procedures, erection tolerances, and nondestructive examination of shop- and field- fabricated welds conforms with Subsections NE-4000 and NE-5000 of the ASME Code.

The containment vessel is designed to permit its construction using large subassemblies. These subassemblies consist of the two heads and three ring sections. Each ring section comprises three courses of plates and is approximately 38 feet high. These are assembled in an area near the final location, using plates fabricated in a shop facility.

3.8.2.7 Testing and Inservice Inspection Requirements

Testing of the containment vessel and the pipe assemblies forming the pressure boundary within the containment vessel will be according to the provisions of NE-6000 and NC-6000 respectively.

Subsection 6.2.5 describes leak-rate testing of the containment system including the containment vessel.

Inservice inspection of the containment vessel will be performed according to the ASME Code Section XI, Subsection IWE, and will be described in the Combined License application.

3.8.7 References

1. D.Bushnell, "BOSOR5 - Program for buckling of elastic-plastic complex shells of revolution including large deflections and creep," Computers and Structures, Vol.6, pp 221-239, 1976

2. C.D Miller, R.B.Grove, J.G.Bennett, "Pressure Testing of Large Scale Torispherical Heads Subject to Knuckle Buckling," NUREG/CP-0065, Transactions of the International Conference on Structure Mechanics in Reactor Technology, August 1985.

3. "Leak and Structural Test of Personnel Airlock for LWR Containments Subjected to Pressures and Temperatures beyond Design Limits," NUREG/CR-5118, SAND88-7155, May 1989.

4. "Analysis of Bellows Expansion Joints in the Sequoyah Containment," NUREG/CR-5561, SAND90-7020, December 1991.

5. "Severe Accident Testing of Electrical Penetration Assemblies," NUREG/CR-5334, SAND89-0327, November 1989.

6. ASTM C 94-1990, "Specifications for Ready-Mixed Concrete."

7. ACI 304R-1989, "Guide for Measuring, Mixing, Transporting, and Placing Concrete."

8. ASTM C 150-1989, "Specification for Portland Cement."

9. ASTM C 33-1990, "Specification for Concrete Aggregates."

10. ASTM C 131-1989, "Resistance to Abrasion of Small Size Coarse Aggregate by Use of the Los Angeles Machine."

11. ASTM C 535-1989, "Test Method for Resistance to Degradation of Large-Size Coarse Aggregate by Abrasion and Impact in the Los Angeles Machine."

12. ASTM D 512-1989, "Chloride Ion in Industrial Water."

13. ASTM D 1888-1978, "Particulate and Dissolved Matter in Industrial Water."

14. ASTM C 618-1989, "Fly Ash and Raw or Calcined Natural Pozzolans for Use in Portland Cement Concrete."

15. ASTM C 311-1990, "Sampling and Testing Fly Ash or Natural Pozzolans for Use as Mineral Admixture in Portland Cement Concrete."

16. ASTM C 260-1986, "Air Entraining Admixtures for Concrete."

17. ASTM C 494-1986, "Chemical Admixtures for Concrete."

18. ACI 211.1-1989, "Standard Practice for Selecting Proportions for Normal, Heavy Weight, and Mass Concrete."

19. ASTM A 615-1990, "Deformed and Plain Billet Steel Bars for Concrete Reinforcement."

20. ASTM A 706-1990, "Low Alloy Steel Deformed Bars for Concrete Reinforcement."

21. ANSYS, Version 4.4. A135 for SILICONGRAPHICS 4D and INDIGO.

22. D. Bushnell, "Elastic-Plastic Buckling of Internally Pressurized Ellipsoidal Pressure Vessel Heads," Welding Research Council Bulletin 267, May 1981.

23. J. G. Bennett, "An Assessment of Loss-of-Containment Potential Because of Knuckle Buckling for 4:1 Steel Containment Heads," NUREG/CR-4926, LA-10972-MS, April 1987 (This Report also includes the Contractor's Report: "Buckling and Rupture Tests of Two Fabricated Torispherical Heads under Internal Pressure," by R. B. Grove, S. W. Peters, C. D. Miller, and M. F. Eder, C.B.I. Industries, Inc. Research Laboratory.)

24. D. Bushnell, "Stress, Stability, and Vibration of Complex Branched Shells of Revolution: Analysis and User's Manual for BOSOR-4," LMSC-D243605, Lockheed Missiles and Space, Palo Alto, Cal., 1972.

25. "Evaluation of Seals for Mechanical Penetrations of Containment Buildings", NUREG/CR-5096 SAND88-7016.

26. "Experimental Results from Containment Piping Bellows Subjected to Severe Accident Conditions", NUREG/CR-6154, SAND94-1711, Vol. 1,September, 1994

Table 3.8.2-1

LOAD COMBINATIONS AND SERVICE LIMITS FOR CONTAINMENT VESSEL

Load Description		Load Combination and Service Limit										
		Con	Test	Des.	Des.	A	A	A	C	C	C	D
Dead	D	x	x	x	x	x	x	x	x	x	x	x
Live	L	x	x	x	x	x	x	x	x	x	x	x
Wind	W	x				x						
SSE	E_s								x	x		x
Tornado	W_t										x	
Test pressure	P_t		x									
Test temperature	T_t		x									
Operating pressure	P_o					x				x	x	
Design pressure	P_d			x			x		x			x
External pressure (3.0 psid)	P_e				x			x		x		
Normal reaction	R_o				x	x		x		x	x	
Normal thermal	T_o				x	x		x		x	x	
Accident thermal reactions	R_a			x			x		x			x
Accident thermal	T_a			x			x		x			x
Accident pipe reactions	Y_r											x
Jet impingement	Y_j											x
Pipe impact	Y_m											x

Notes:

1. Service limit levels are per ASME-NE.
2. Where any load reduces the effects of other loads, that load shall be taken as zero, unless it can be demonstrated that the load is always present or occurs simultaneously with the other loads.

DRAFT

Table 3.8.2-2

CONTAINMENT VESSEL PRESSURE CAPABILITIES

Containment Element	Pressure Capability				
	Deterministic Severe Accident Capacity[1]			Maximum Pressure Capability[2]	
Temperature	100°F	280°F	400°F	100°F	400°F
Cylinder	125 psig	110 psig	104 psig	144 psig	120 psig
Ellipsoidal Head	104 psig	92 psig	87 psig	174 psig	145 psig
22 foot equipment hatch	117 psig	114 psig	110 psig	195 psig	184 psig
16 foot equipment hatch	96 psig	93 psig	90 psig	160 psig	151 psig
Personnel airlocks[3]	>163 psig	>163 psig	>163 psig	>300 psig	>300 psig

Note:

1. The buckling capacity of the ellipsoidal head is taken as sixty percent of the critical buckling pressure calculated by the BOSOR-5 non-linear analyses; the buckling capacity at higher temperatures is calculated by reducing the capacity at 100°F by the ratio of yield at 100°F to yield at the higher temperature. Evaluations of the other elements are according to ASME Service Level C and include use of Code Case N284.

2. The estimated maximum pressure capability is based on minimum specified material properties.

3. The capacities of the personnel airlock are estimated from test results.

Table 3.8.2-3

ANALYSIS AND TEST RESULTS OF FABRICATED HEADS (Reference 23)

	Test Model #1	Test Model #2
Cylinder radius	96.0 inches	96.0 inches
Knuckle radius	32.64 inches	32.64 inches
Spherical radius	172.8 inches	172.8 inches
Thickness	0.196 inches	0.27 inches
Head height/radius	0.5	0.5
Radius/thickness	490	356
Test initial buckling pressure	58 psig	106 psig
Test collapse pressure	229 psig	332 psig
Collapse pressure/initial buckling pressure	3.95	3.13
BOSOR-5 predicted buckling pressure	73.6 psig	106.6 psig

Table 3.8.2-4

SUMMARY OF CONTAINMENT VESSEL MODELS AND ANALYSIS METHODS

Model	Analysis Method	Program	Purpose
Axisymmetric shell	Modal analysis	CBI / Kalnins	To calculate frequencies and mode shapes for comparison against stick model
Lumped mass stick model	Modal analysis	CBI / SAP	To create equivalent stick model for use in nuclear island seismic analyses
Axisymmetric shell	Static analyses using Fourier harmonic loads	CBI / Kalnins	To calculate containment vessel shell stresses
Axisymmetric shell	Non-linear bifurcation	BOSOR5	To calculate buckling capacity close to base under thermal loads. To calculate pressure capacity of top head.
Finite element shell	Linear bifurcation	ANSYS 5.1	To study local effect of large penetrations and embedment on buckling capacity for axial and external pressure loads
Finite element shell	Modal analysis	ANSYS 5.1	To calculate frequencies and mode shapes for local effects of equipment hatches and personnel airlocks
Finite element shell	Static analyses	ANSYS 5.1	To calculate local shell stress in vicinity of the equipment hatches and personnel airlocks

DRAFT

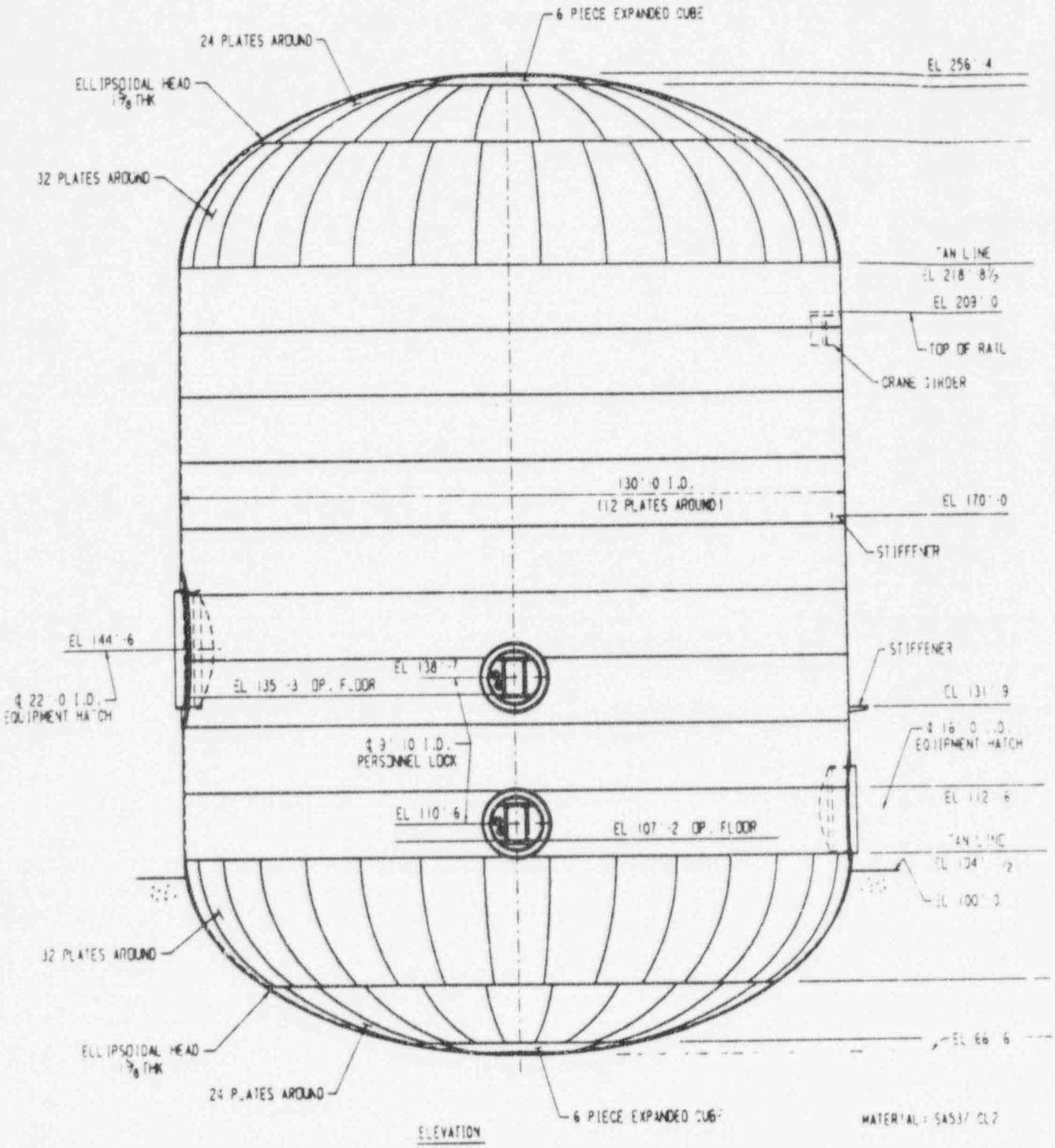

ELEVATION

Figure 3.8.2-1 (Sheet 1 of 4)

Containment Vessel General Outline

DRAFT

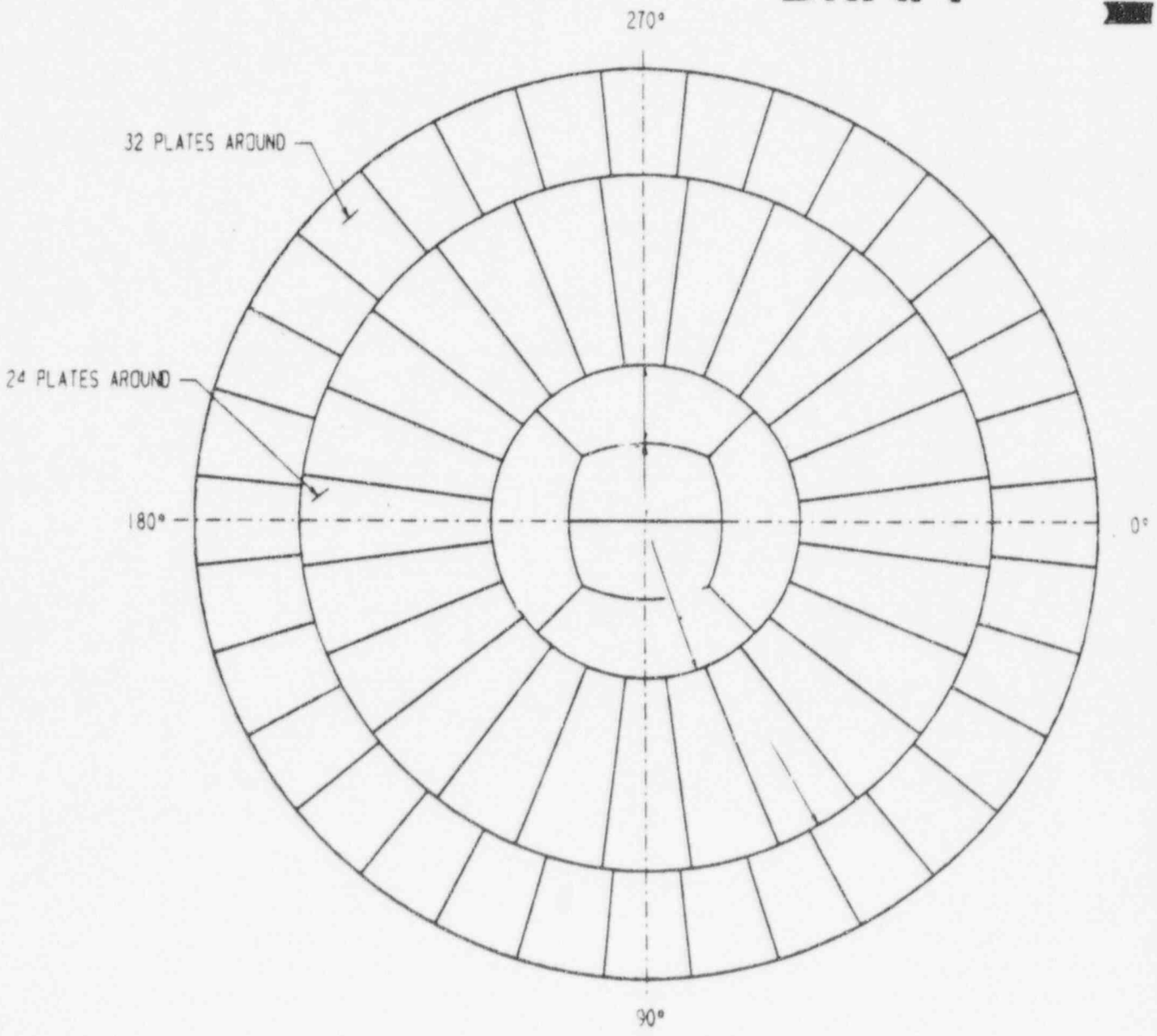

TOP AND BOTTOM HEAD LAYOUT

Figure 3.8.2-1 (Sheet 2 of 3)

Containment Vessel General Outline

DRAFT

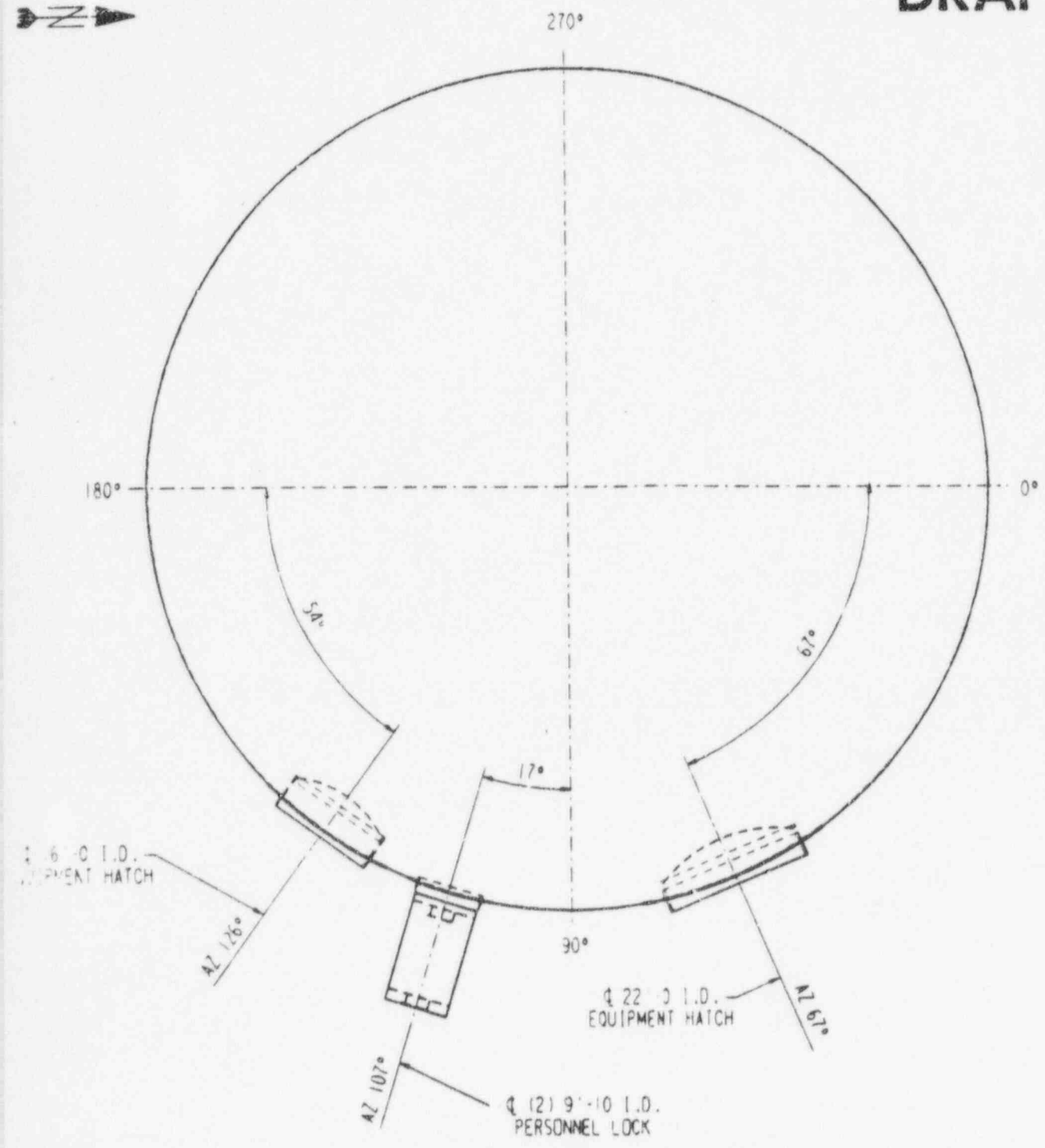

ORIENTATION OF MAJOR PENETRATIONS

Figure 3.8.2-1 (Sheet 3 of 4)

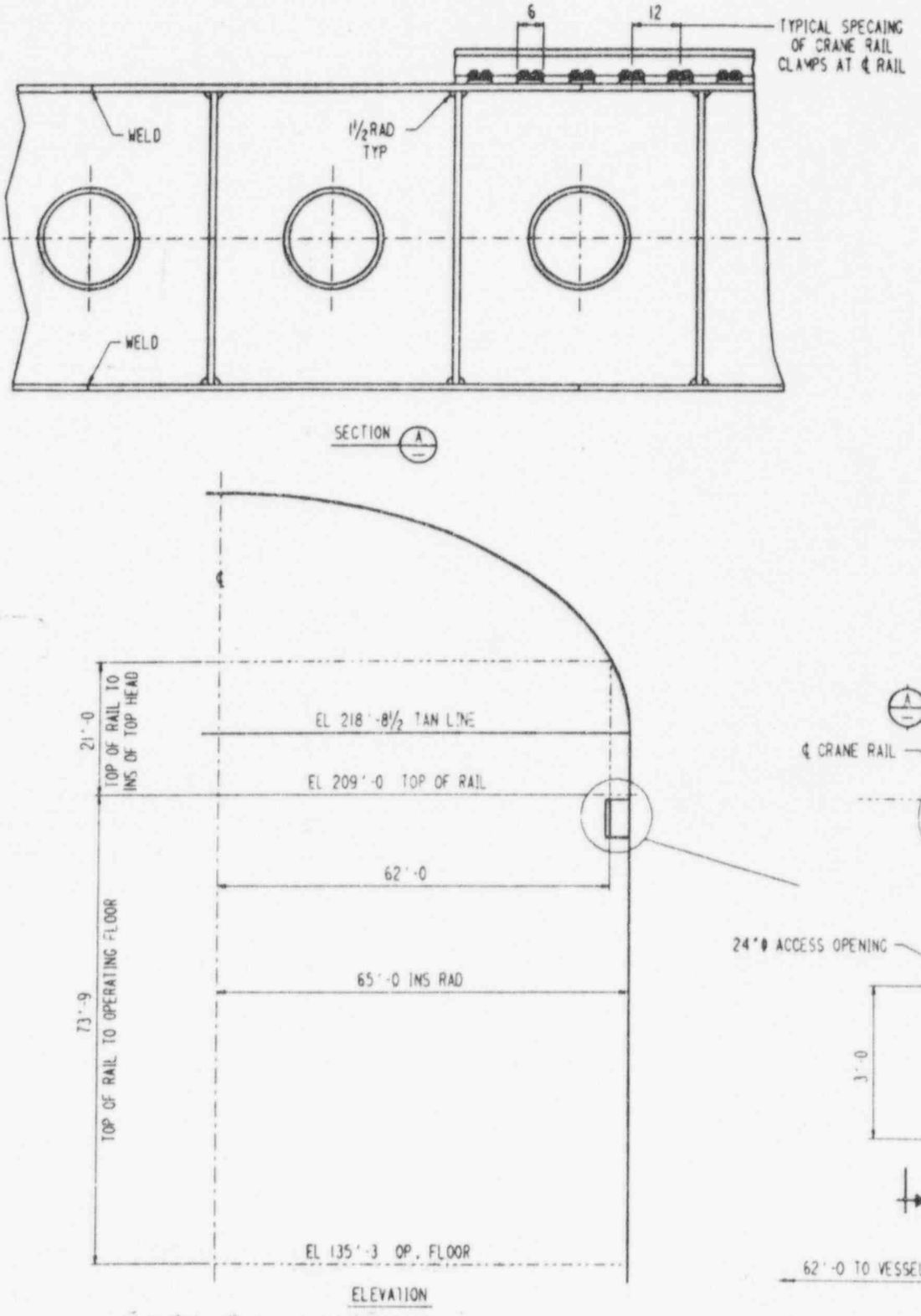
6
12
TYPICAL SPECAING OF CRANE RAIL CLAMPS AT ℄ RAIL
WELD
1½ RAD TYP
WELD
SECTION A
21'-0
TOP OF RAIL TO INS OF TOP HEAD
EL 218'-8½ TAN LINE
EL 209'-0 TOP OF RAIL
62'-0
73'-9
TOP OF RAIL TO OPERATING FLOOR
65'-0 INS RAD
EL 135'-3 OP. FLOOR
ELEVATION
℄ CRANE RAIL
24'-0 ACCESS OPENING
3'-0
8
62'-0 TO VESSEL ℄

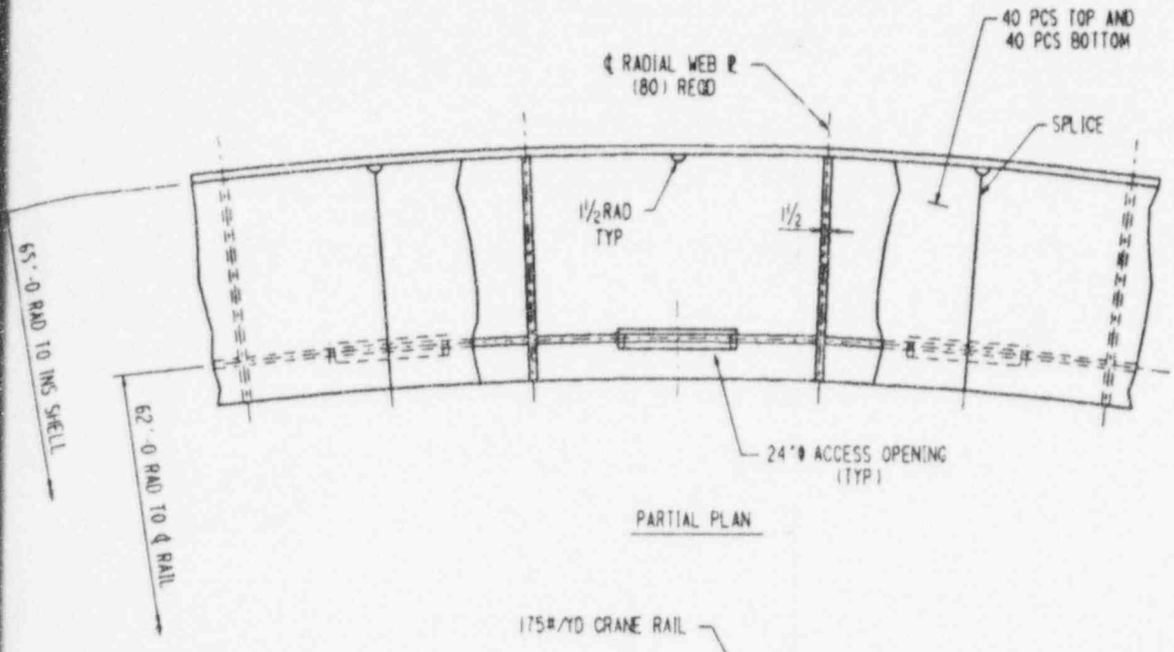

PARTIAL PLAN

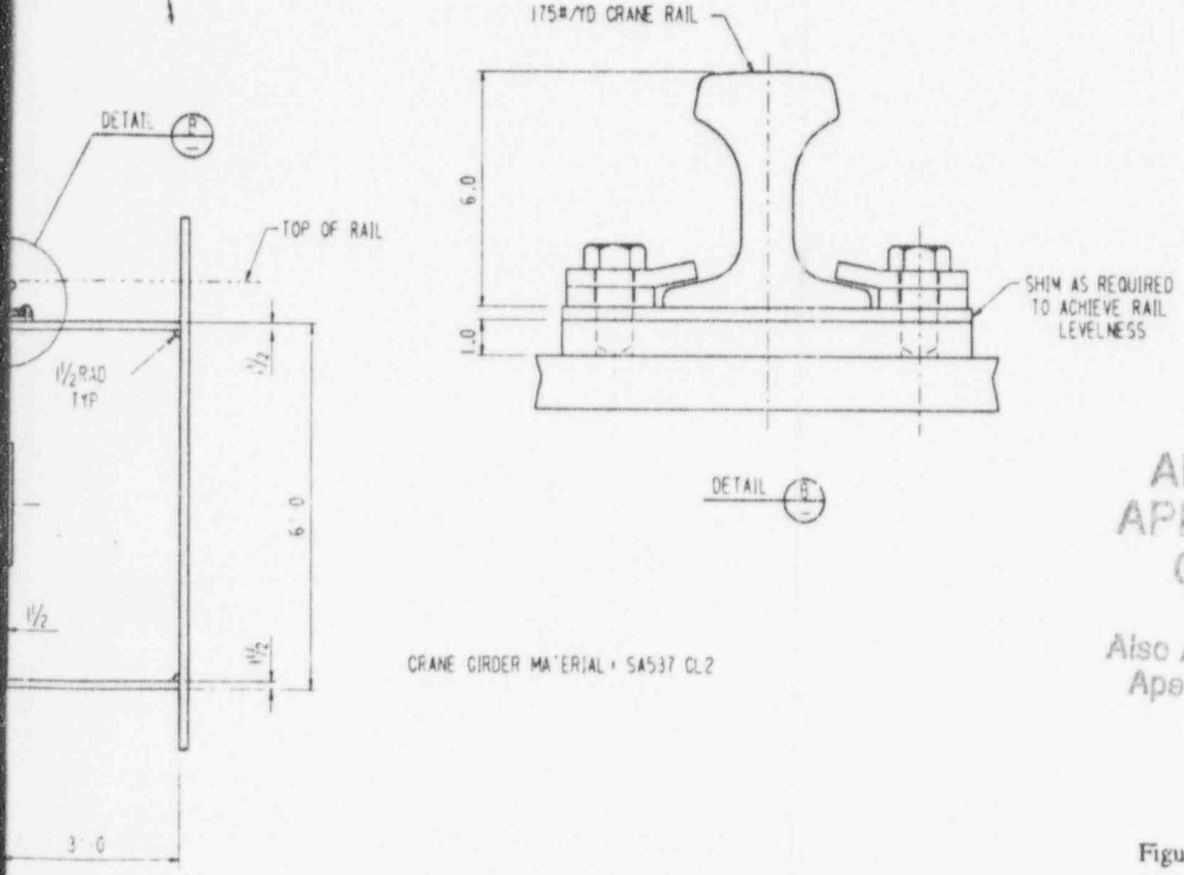

CRANE GIRDER MATERIAL : SA537 CL2

Figure 3.8.2-1 (Sheet 4 of 4)

9601160184-01

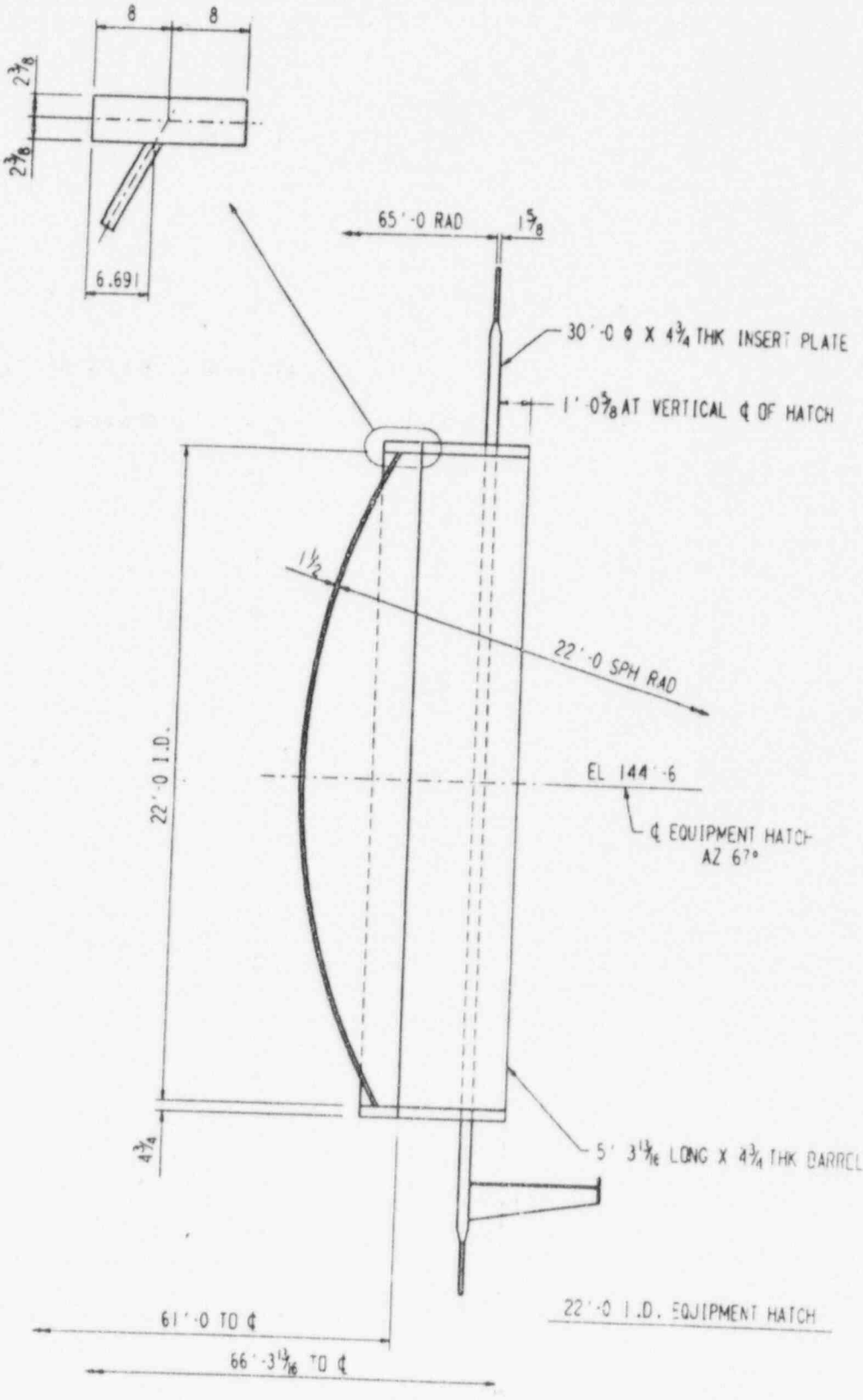
8
8
2 3/8
2 3/8
6.691
65'-0 RAD
1 3/8
30'-0 ϕ X 4 3/4 THK INSERT PLATE
1'-0 3/8 AT VERTICAL ℄ OF HATCH
1 1/2
22'-0 SPH RAD
22'-0 I.D.
EL 144'-6
℄ EQUIPMENT HATCH
AZ 67°
4 3/4
5' 3 13/16 LONG X 4 3/4 THK BARREL
61'-0 TO ℄
66'-3 13/16 TO ℄
22'-0 I.D. EQUIPMENT HATCH

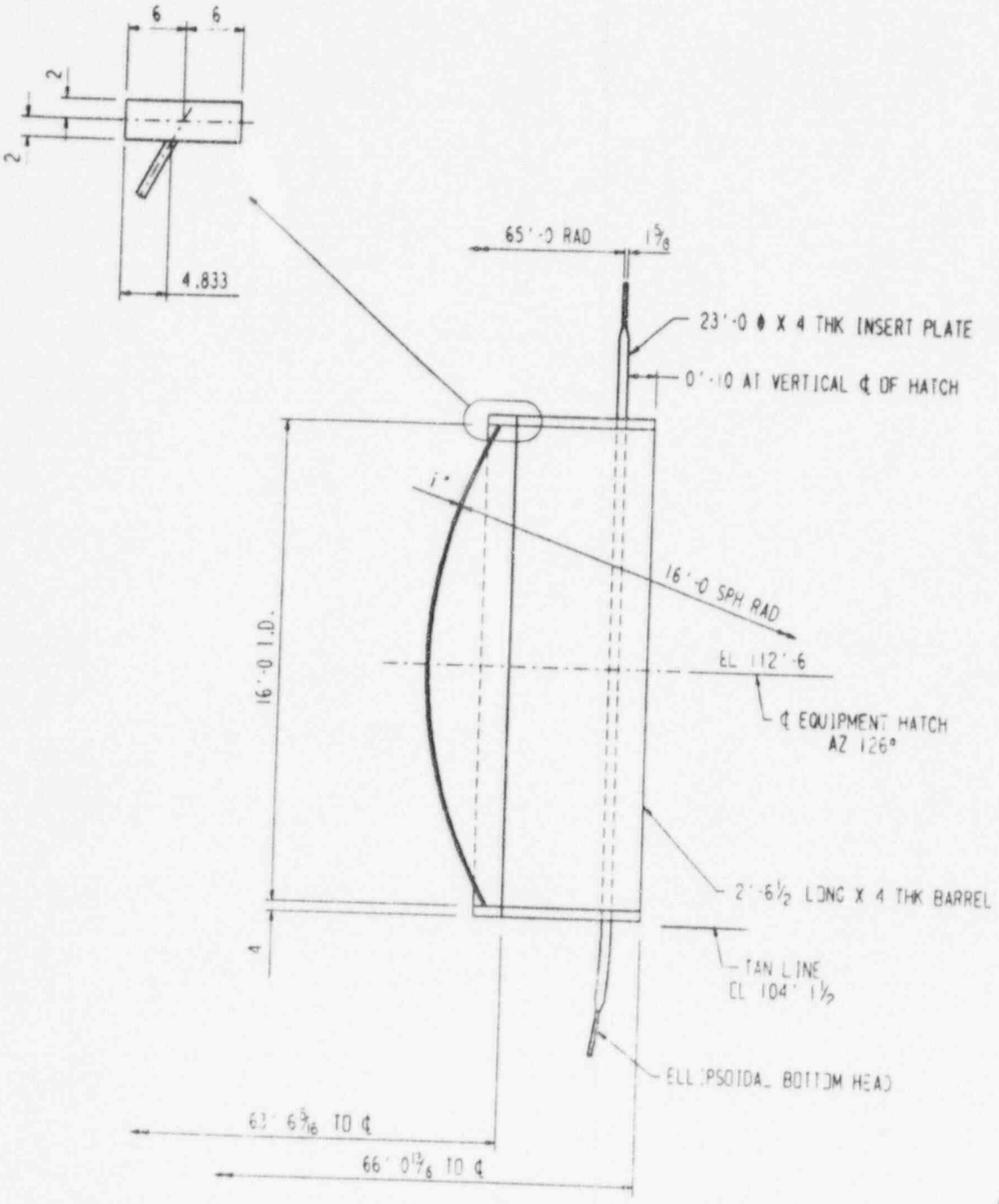

16'-0 I.D. EQUIPMENT HATCH

MATERIAL : SA533 CL.2

Figure 3.8.2-2

Equipment Hatches

9601160184-02

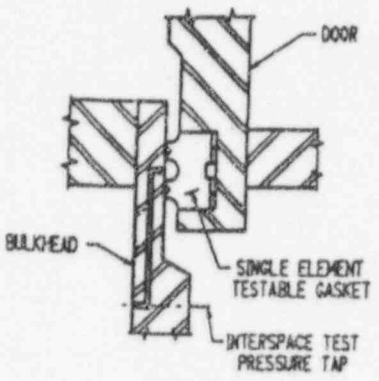

DOOR GASKET CONFIGURATION

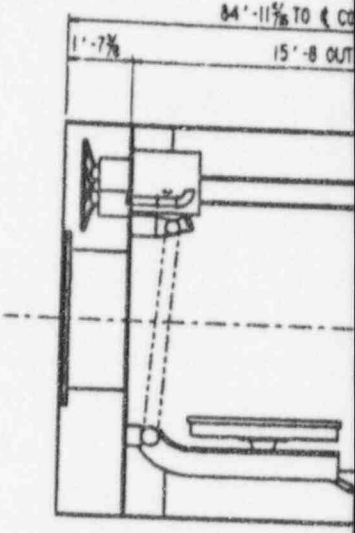

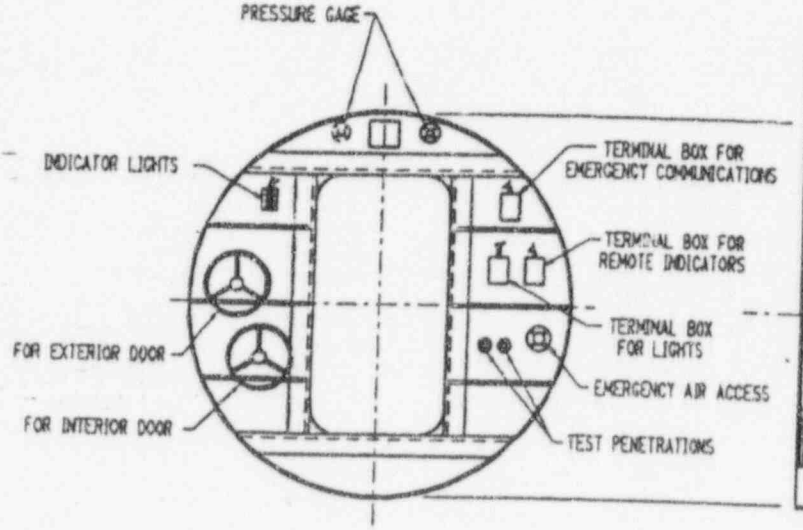

EXTERIOR END VIEW

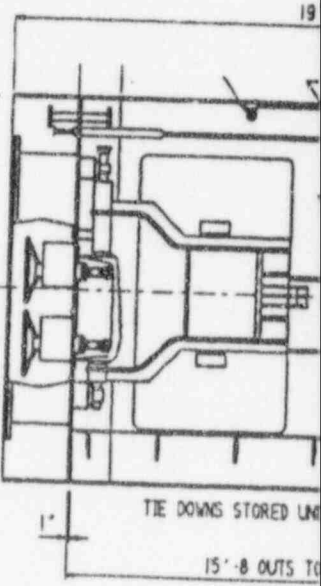

DRAFT

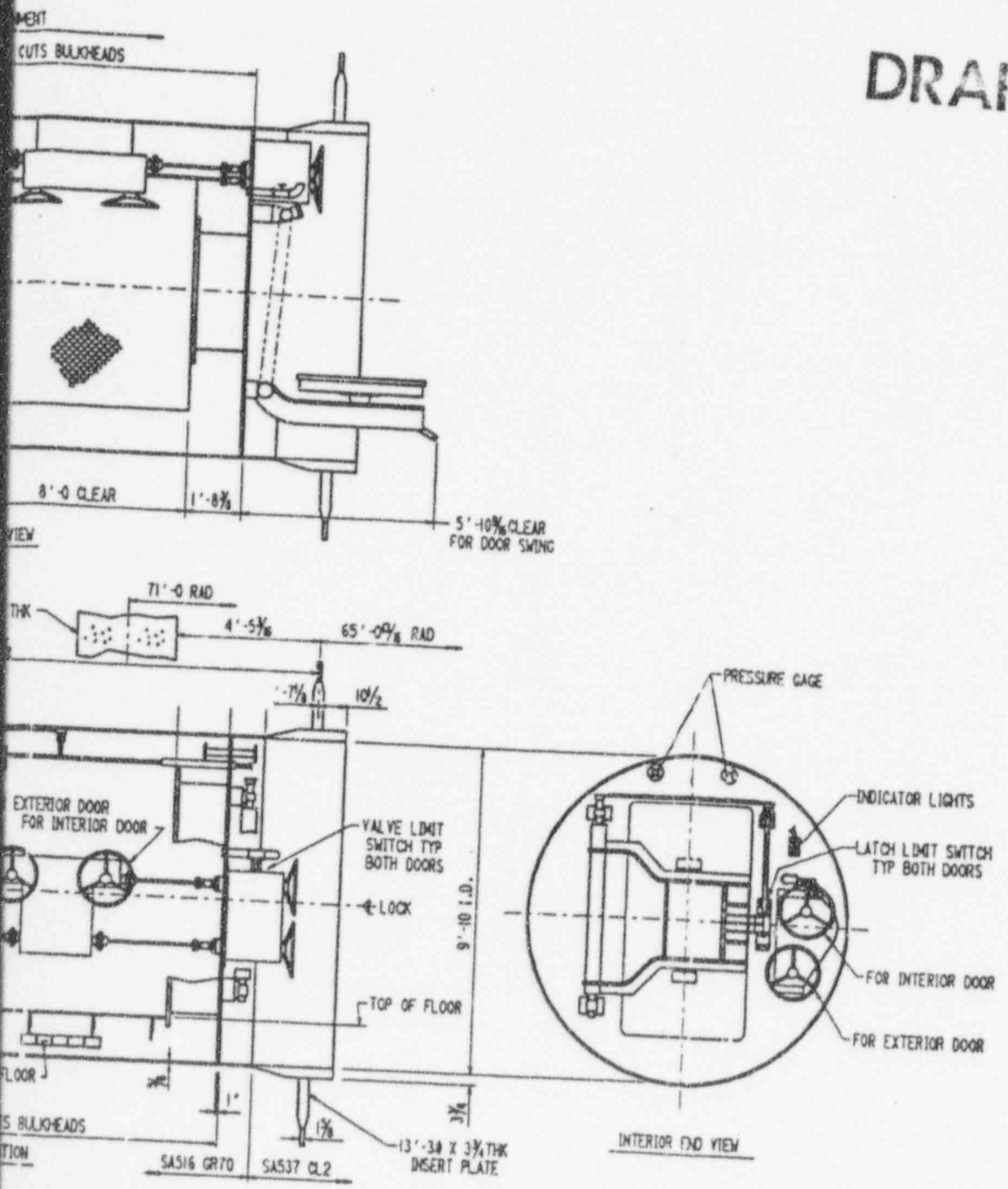

Figure 3.8.2-3

Personnel Airlock

DRAFT

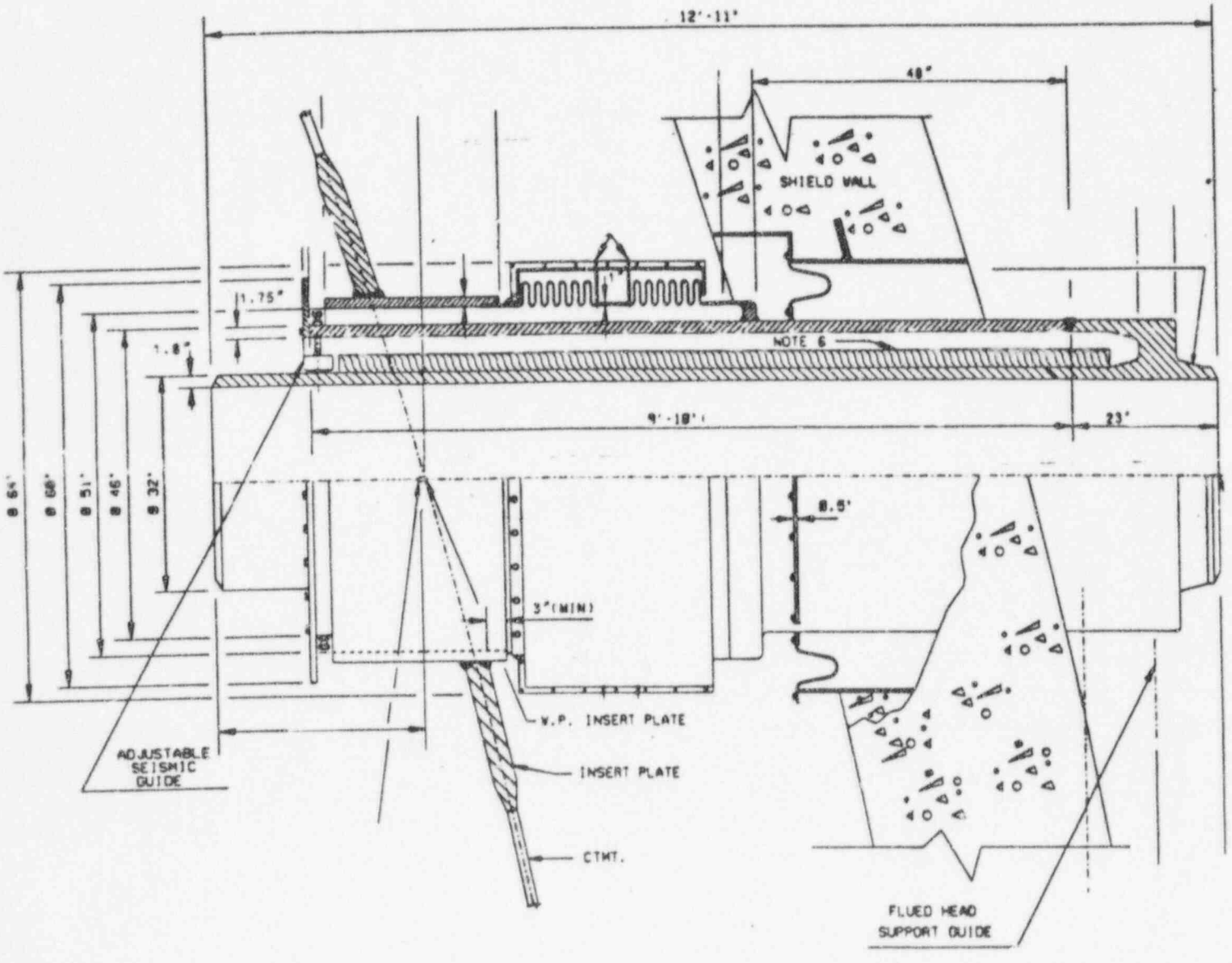

MAIN STEAM PENETRATION

FIGURE 3.8.2-4 SHEET 1 OF 6
CONTAINMENT PENETRATIONS

DRAFT

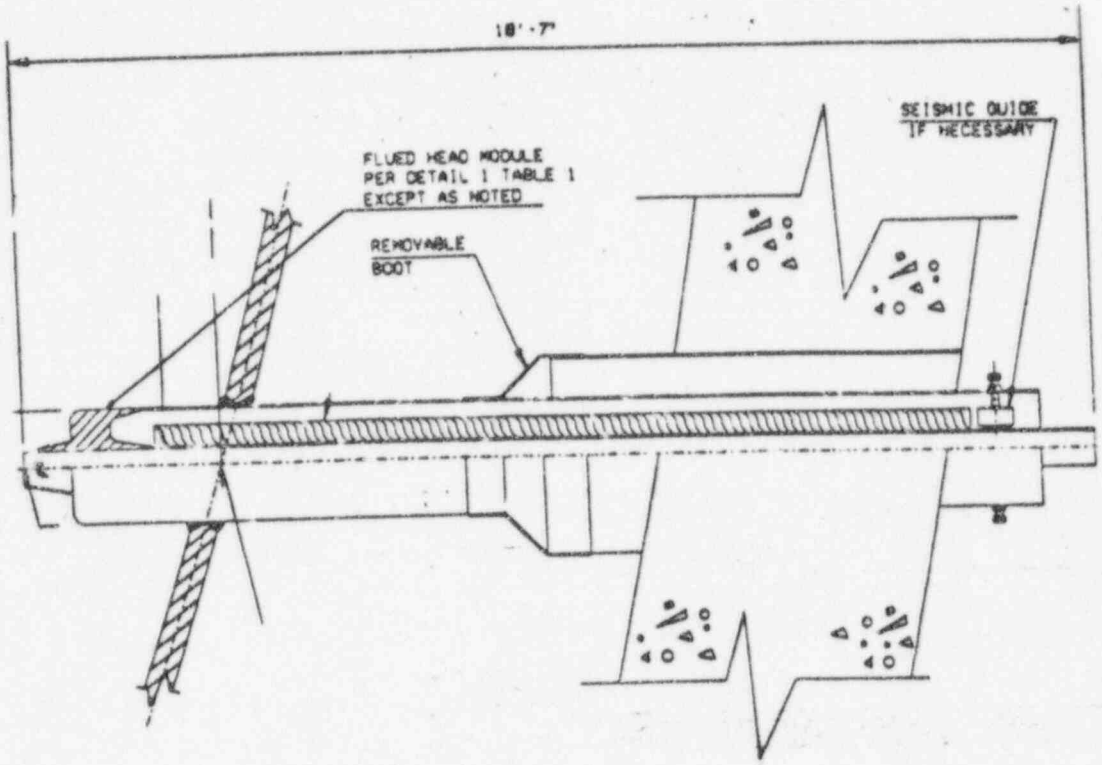

STARTUP FEEDWATER PENETRATION

FIGURE 3.8.2-4 (SHEET 20
CONTAINMENT PENETRATION

DRAFT

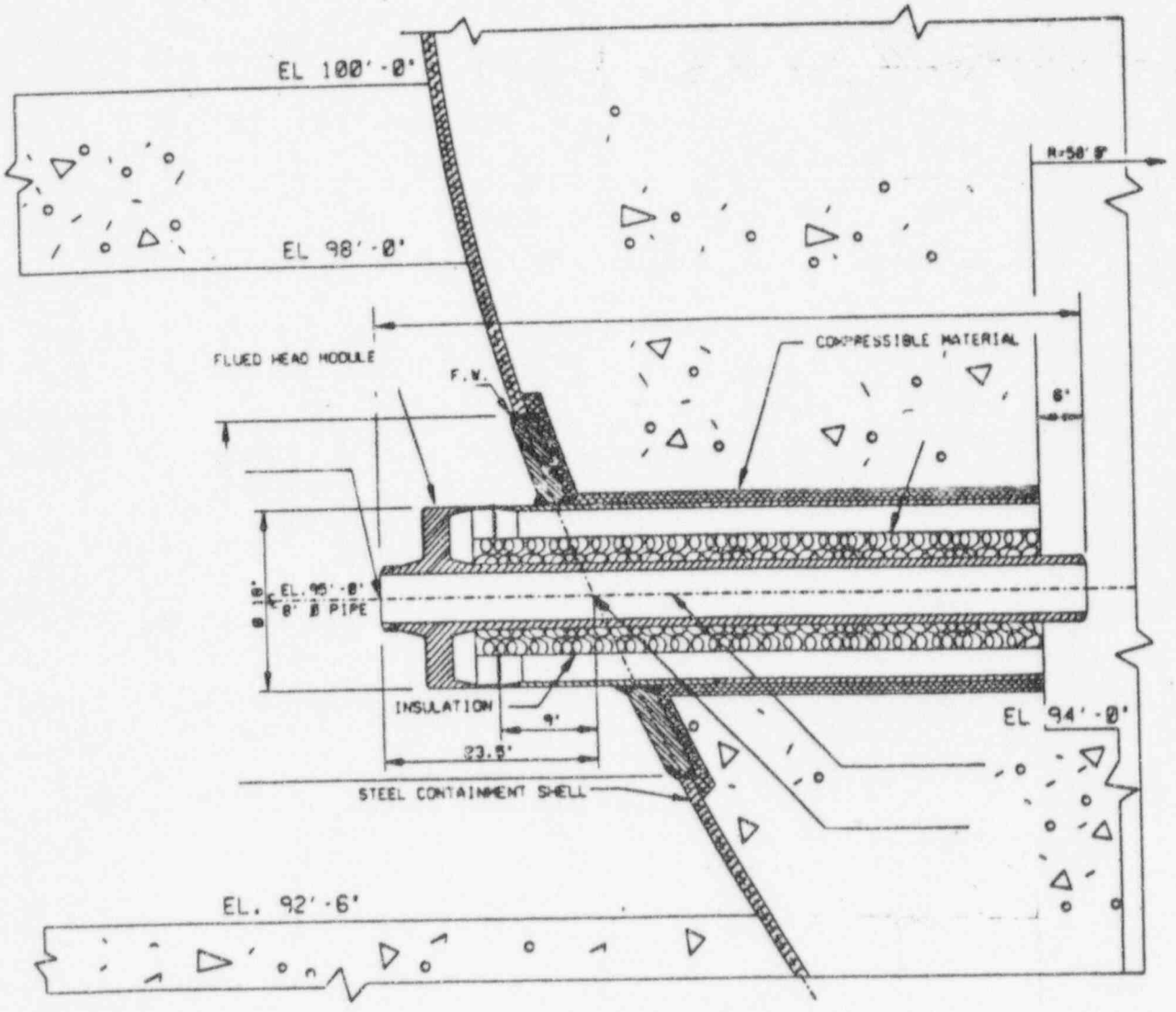

NORMAL RHR PIPING PENETRATION

FIGURE 3.8.2-4 (SHEET 3 OF
CONTAINMENT PENETRATIONS

DRAFT

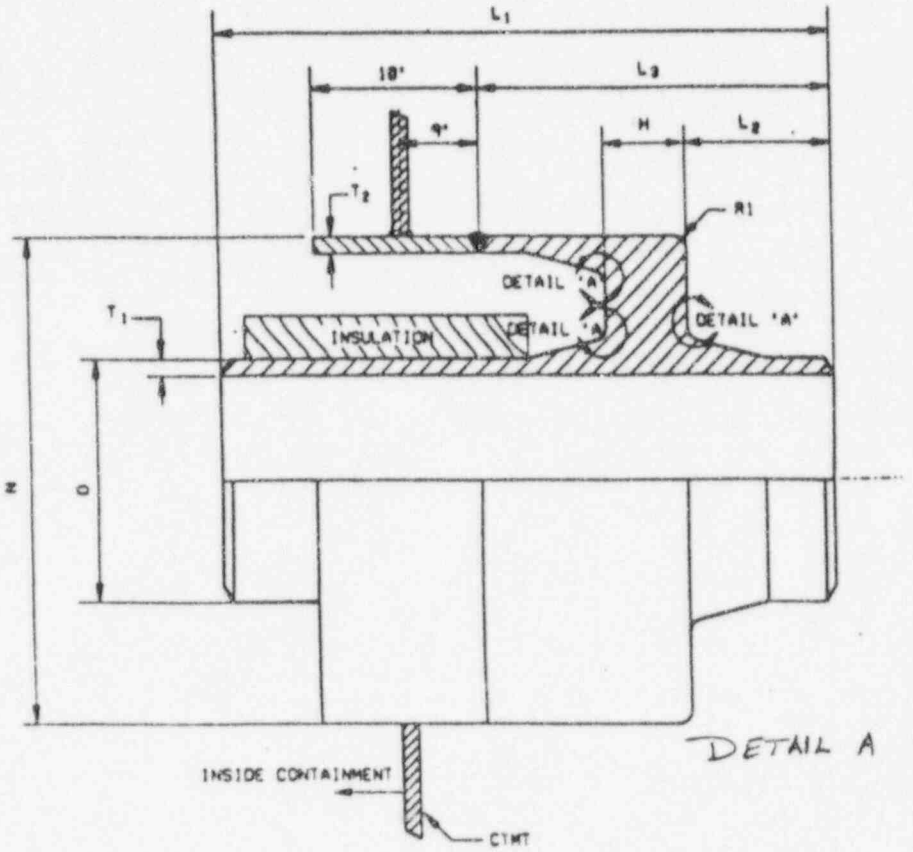

DETAIL A

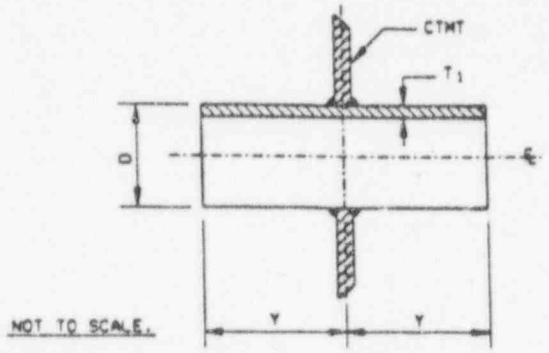

DETAIL B

FIGURE 3.8.2-4 (SHEET 4 OF
CONTAINMENT PENETRATIONS

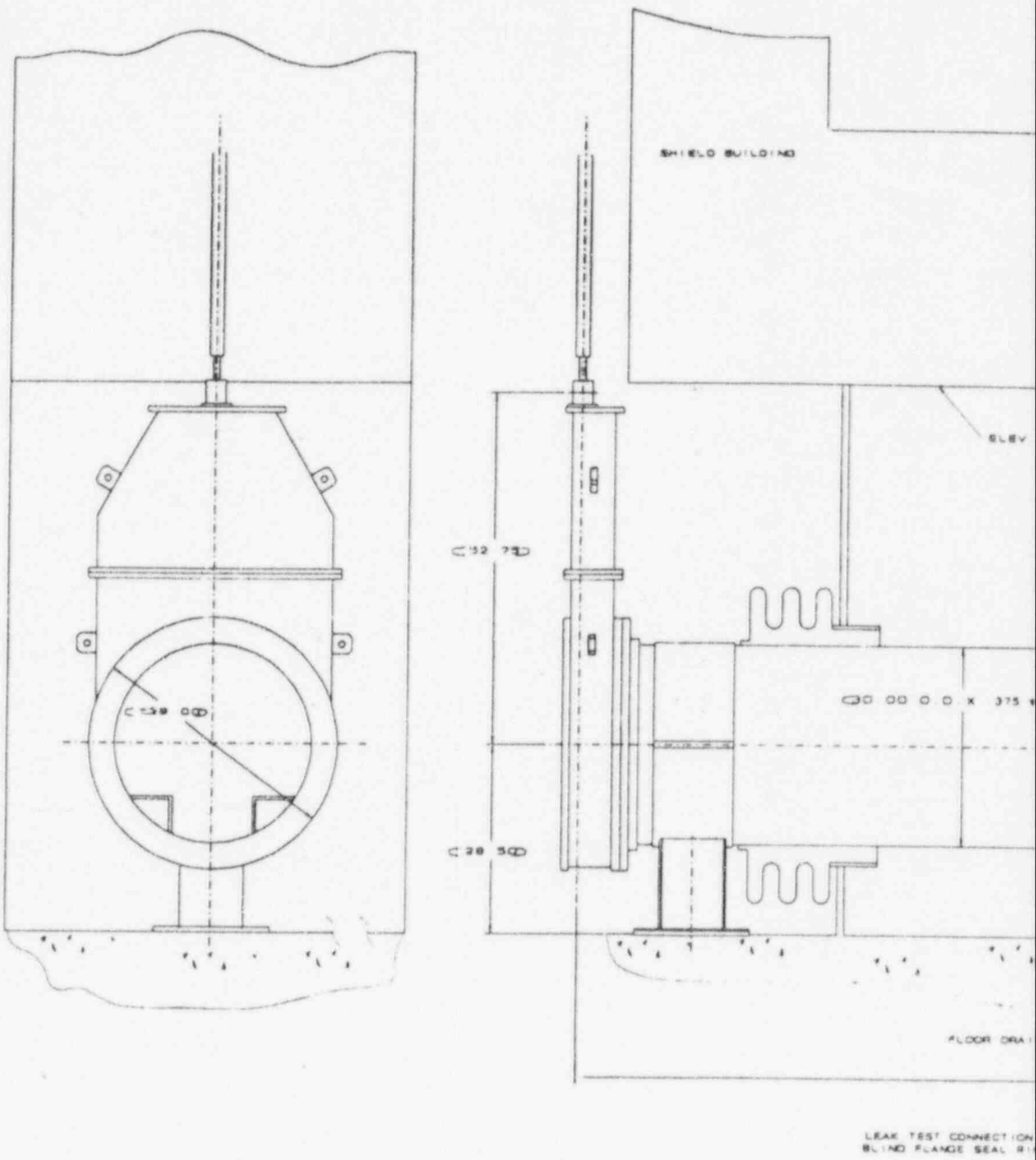
SHIELD BUILDING
ELEV
FLOOR DRA
LEAK TEST CONNECTION
BLIND FLANGE SEAL RI

DRAFT

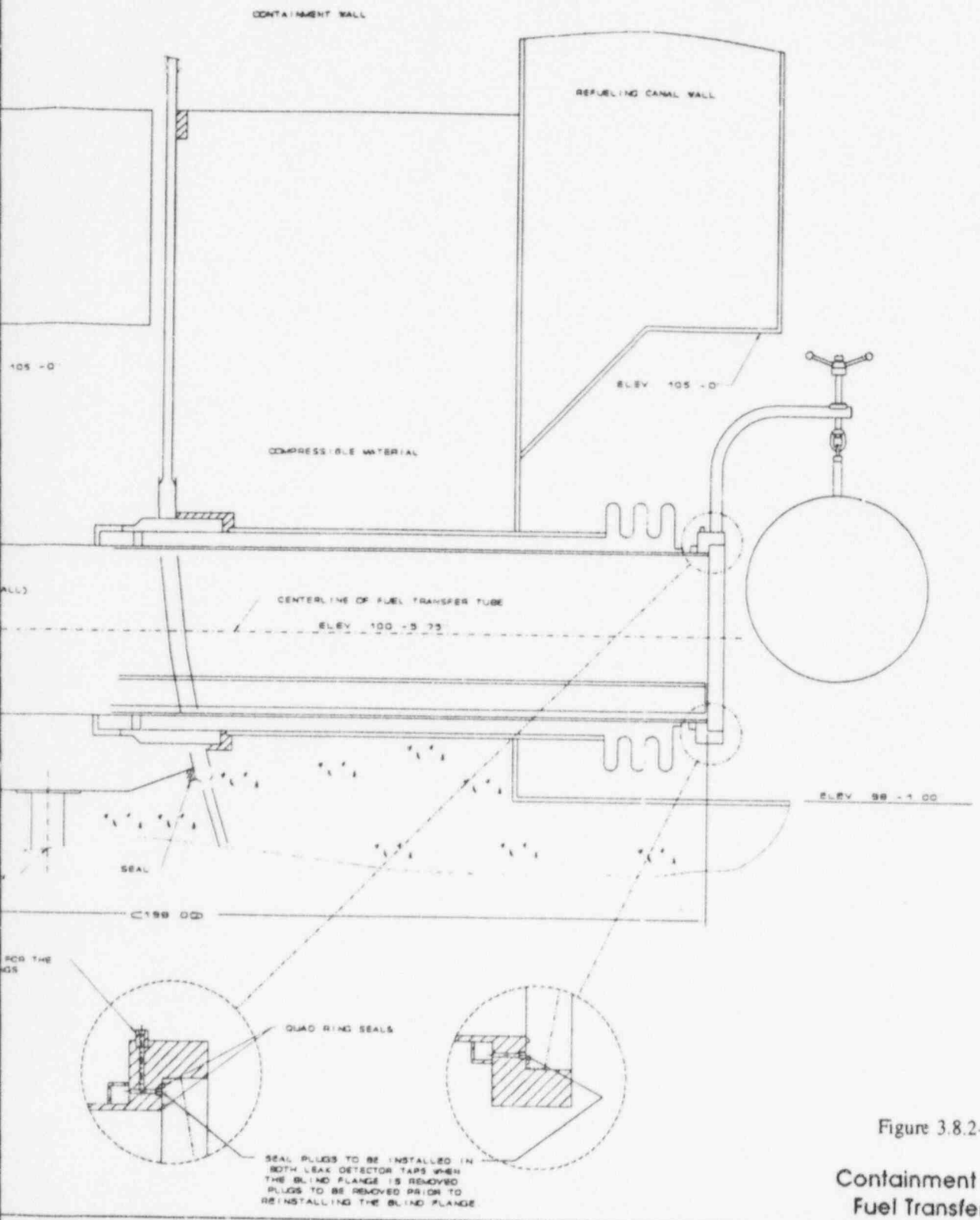

Figure 3.8.2-4 (Sheet ~~7~~ 5 6 of ~~8~~)

Containment Penetrations
Fuel Transfer Penetration

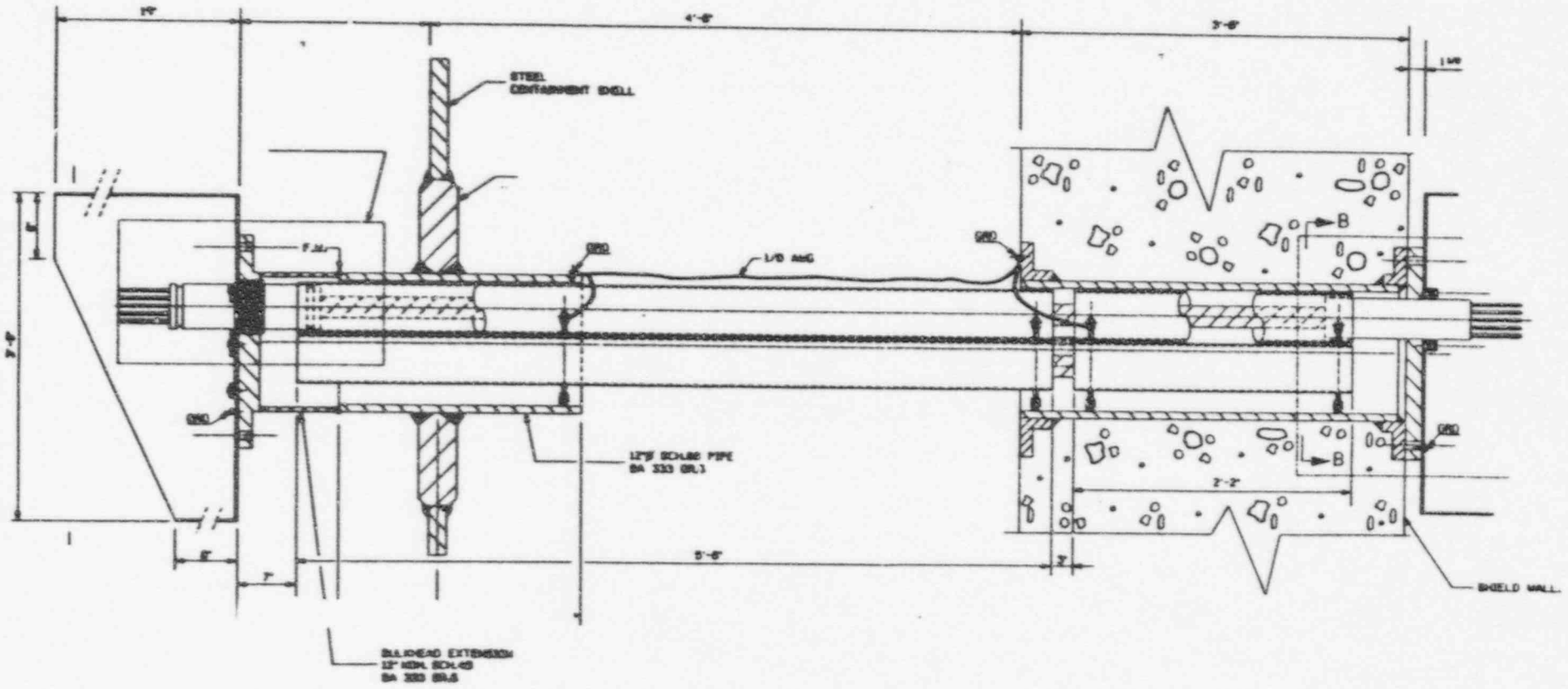

TYPICAL ELECTRICAL PENETRATION

FIGURE 3.8.2-4 (SHEET 6 OF 6)
CONTAINMENT PENETRATIONS

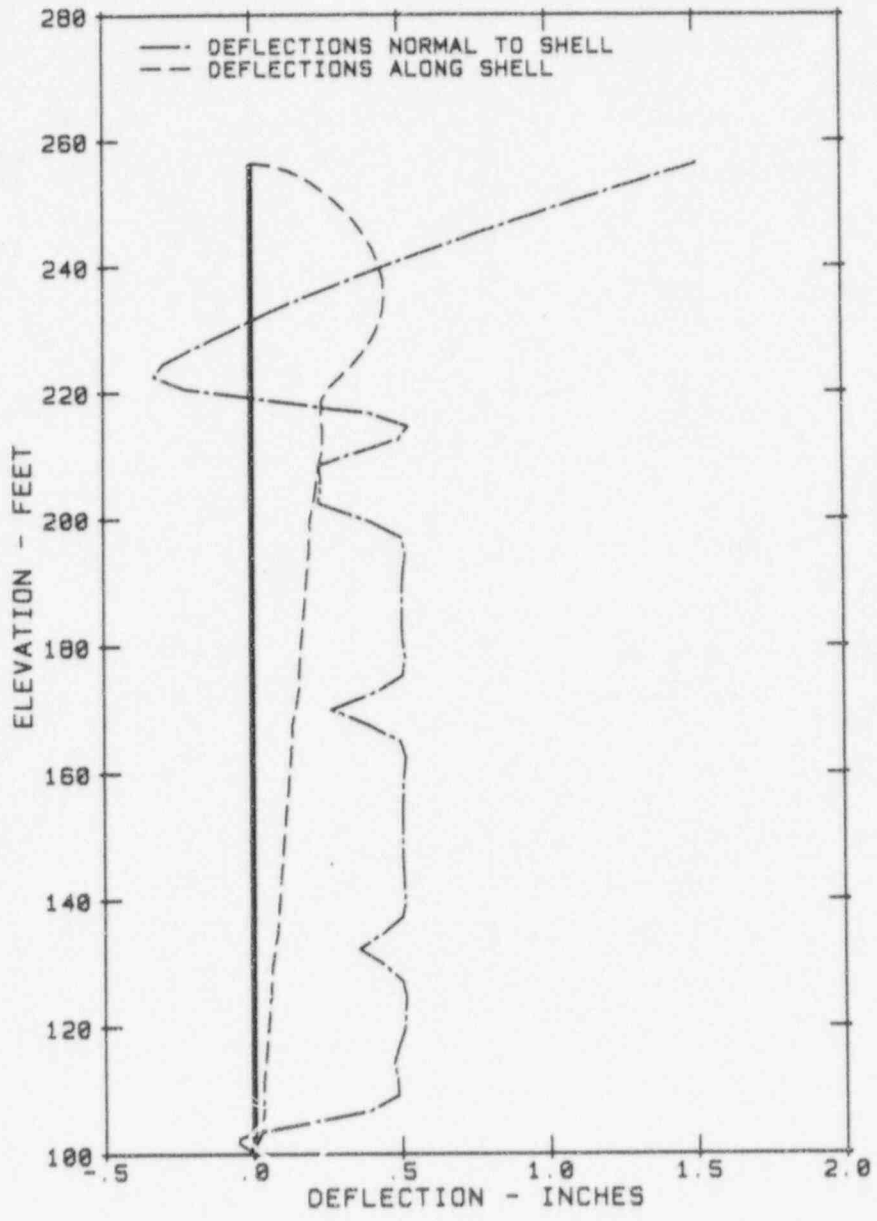

Figure 3.8.2-5 (Sheet 1 of 4)

Containment Vessel Response to Internal Pressure of 45 psig Deflections

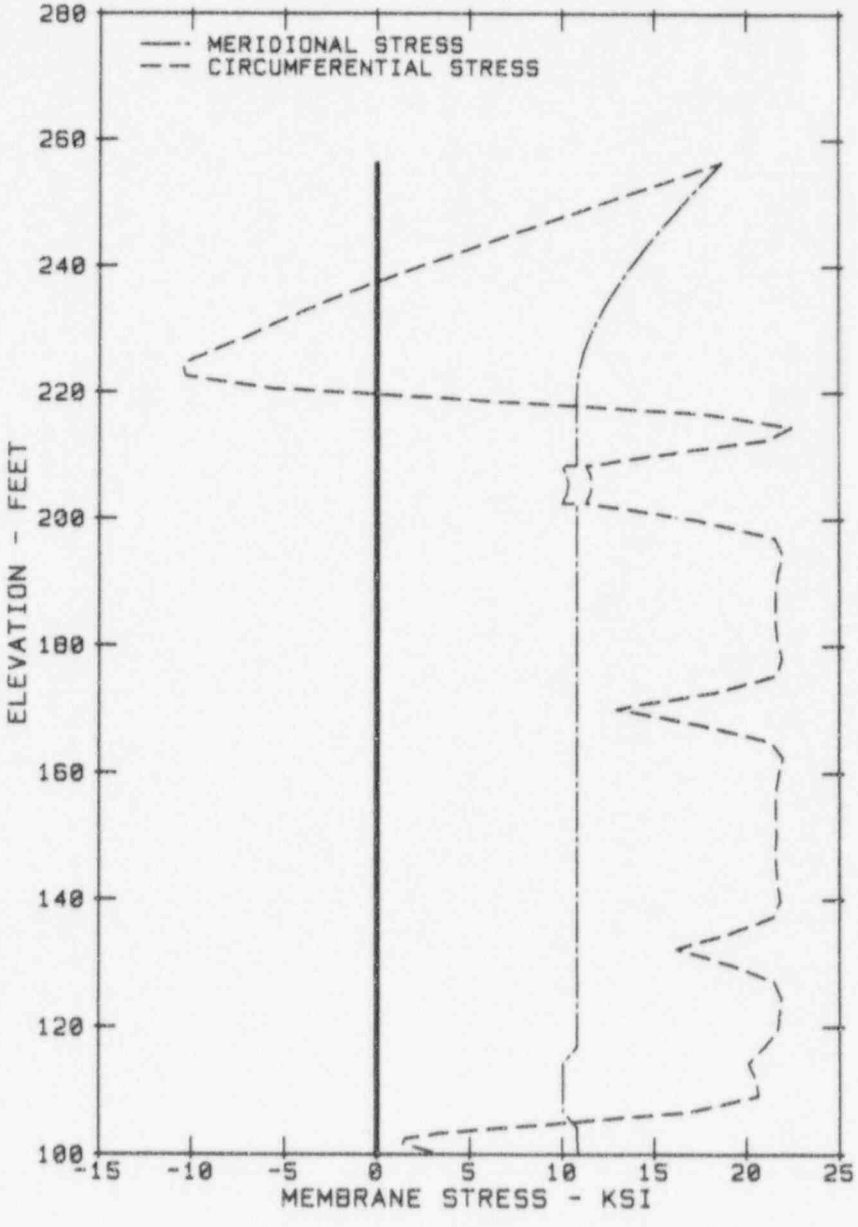

Figure 3.8.2-5 (Sheet 2 of 4)

Containment Vessel Response to Internal Pressure of 45 psig
Membrane Stresses

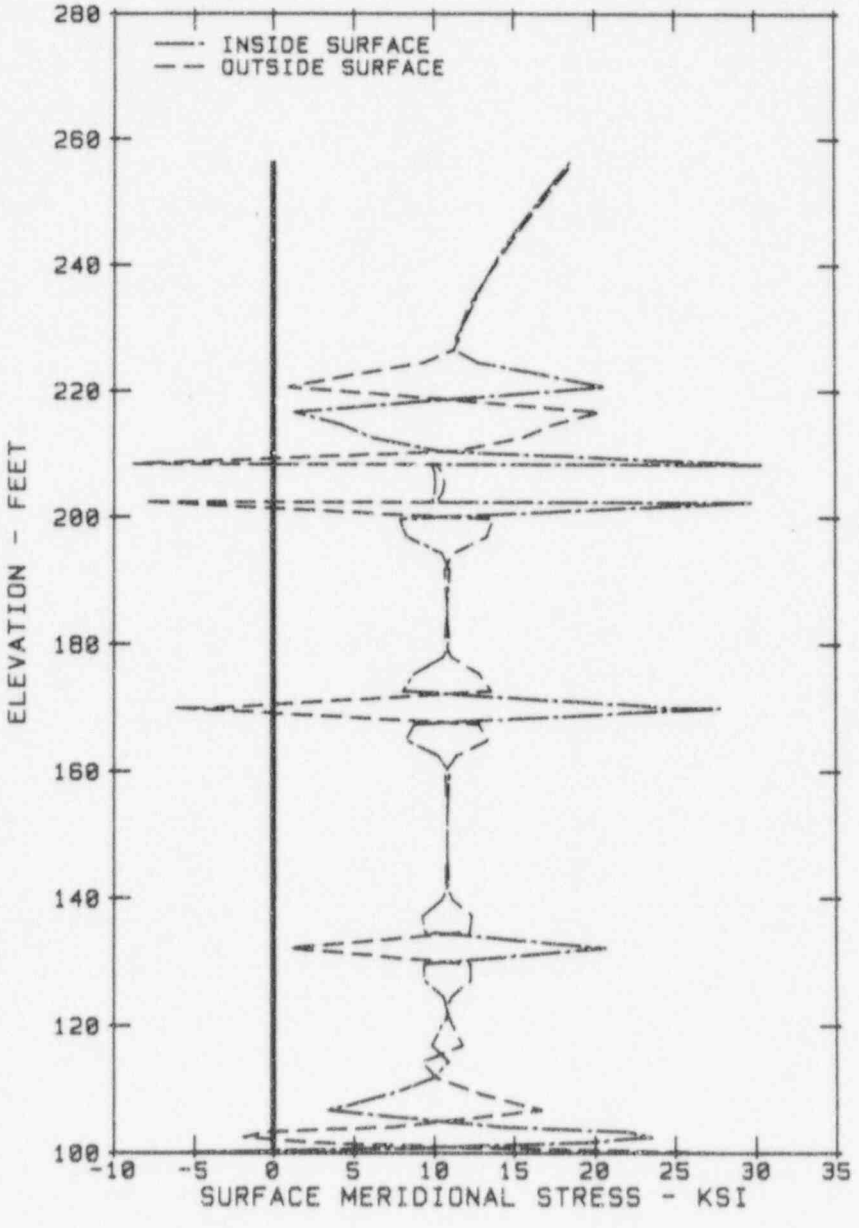

Figure 3.8.2-5 (Sheet 3 of 4)

Containment Vessel Response to Internal Pressure of 45 psig
Surface Meridional Stress

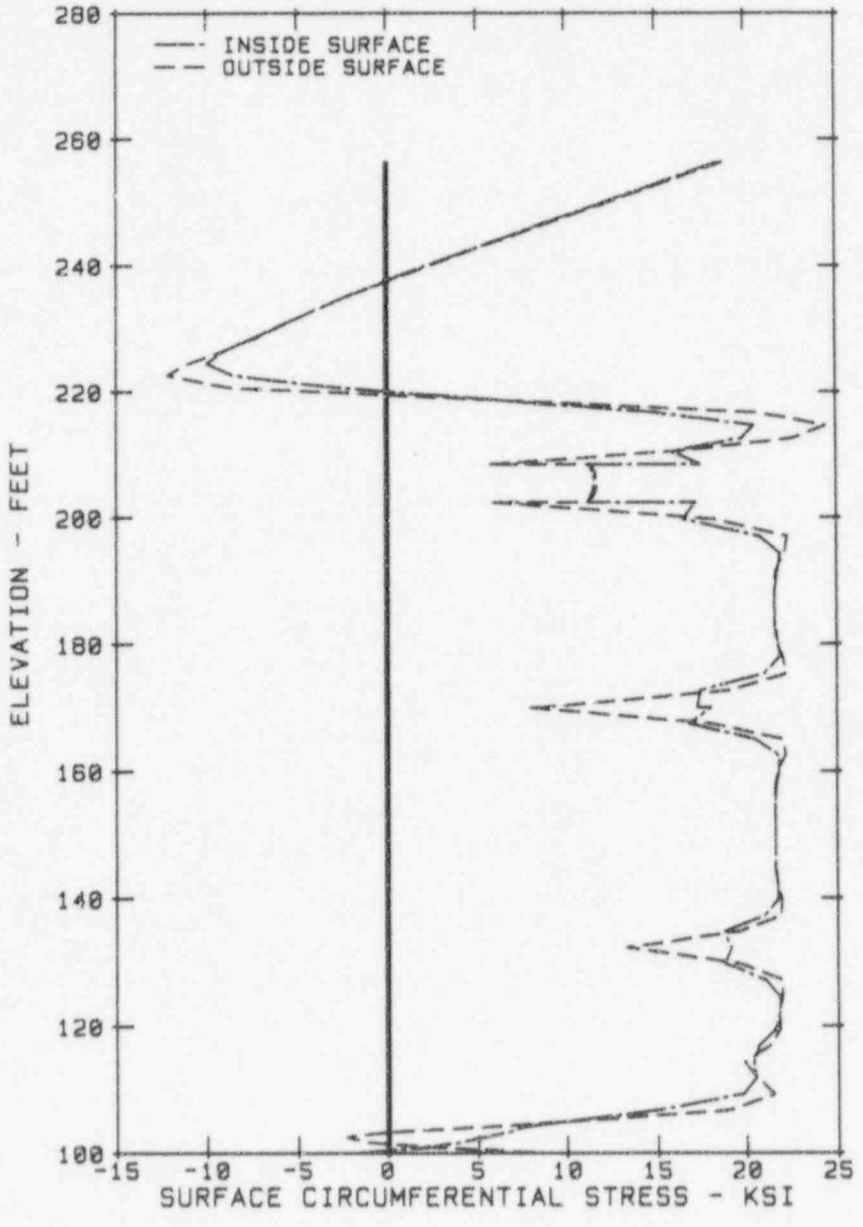

Figure 3.8.2-5 (Sheet 4 of 4)

Containment Vessel Response to Internal Pressure of 45 psig
Surface Circum. Stresses

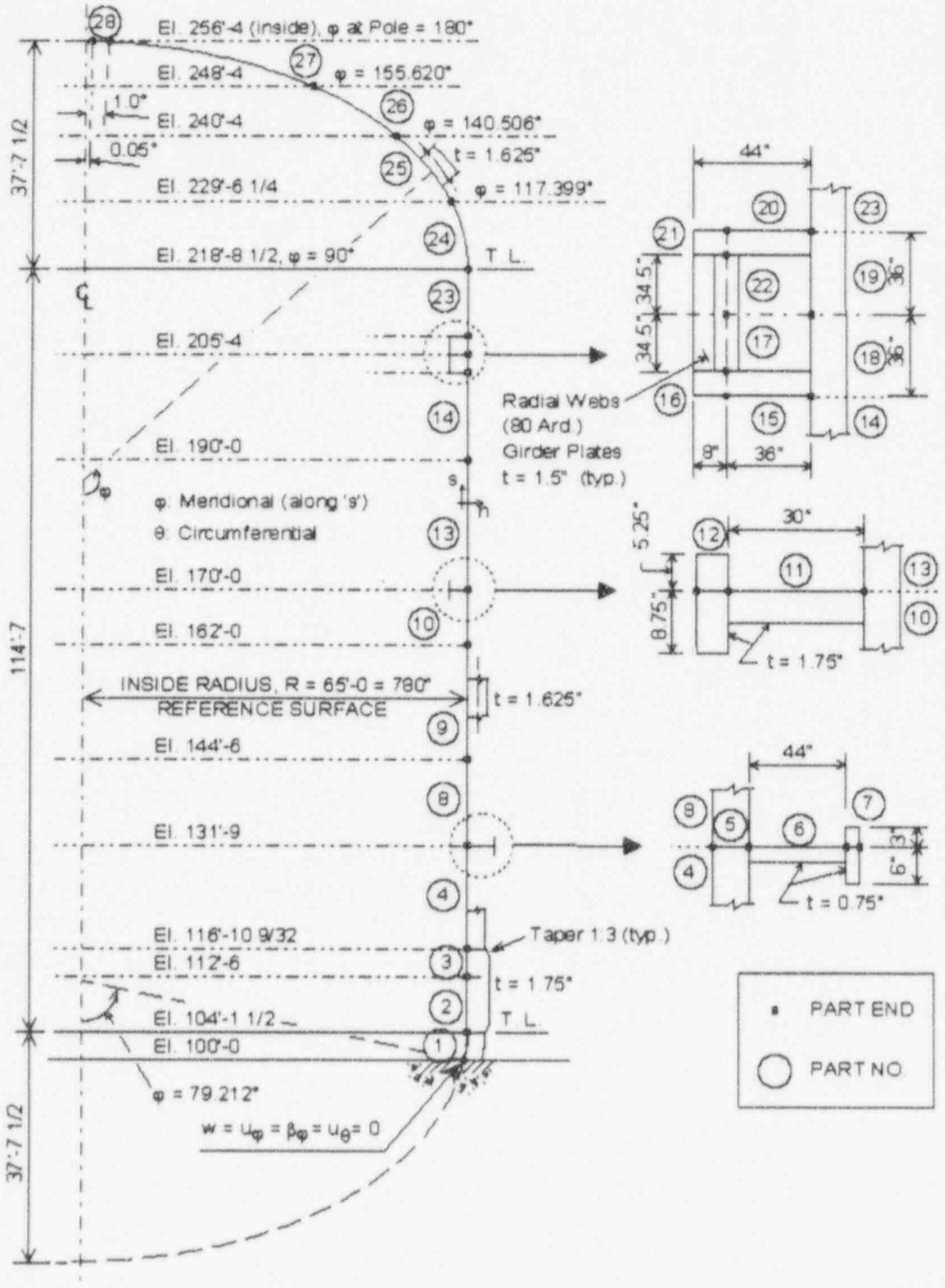

Figure 3.8.2-6

Containment Vessel Axisymmetric Model

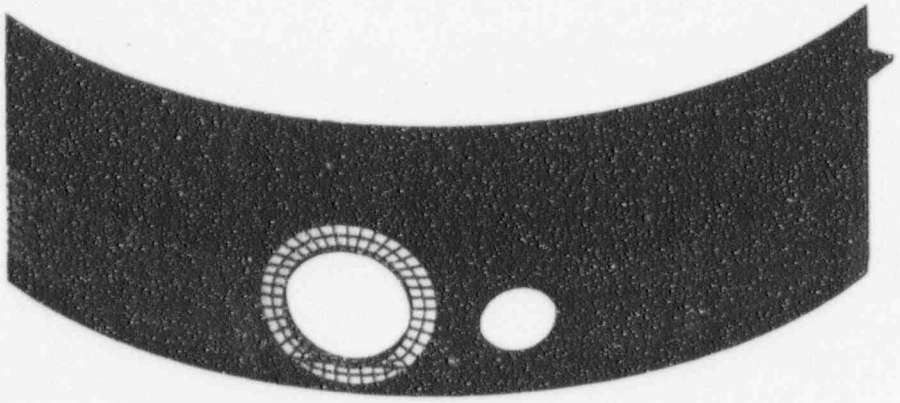

Figure 3.8.2-7

Finite Element Model for Local Buckling Analyses

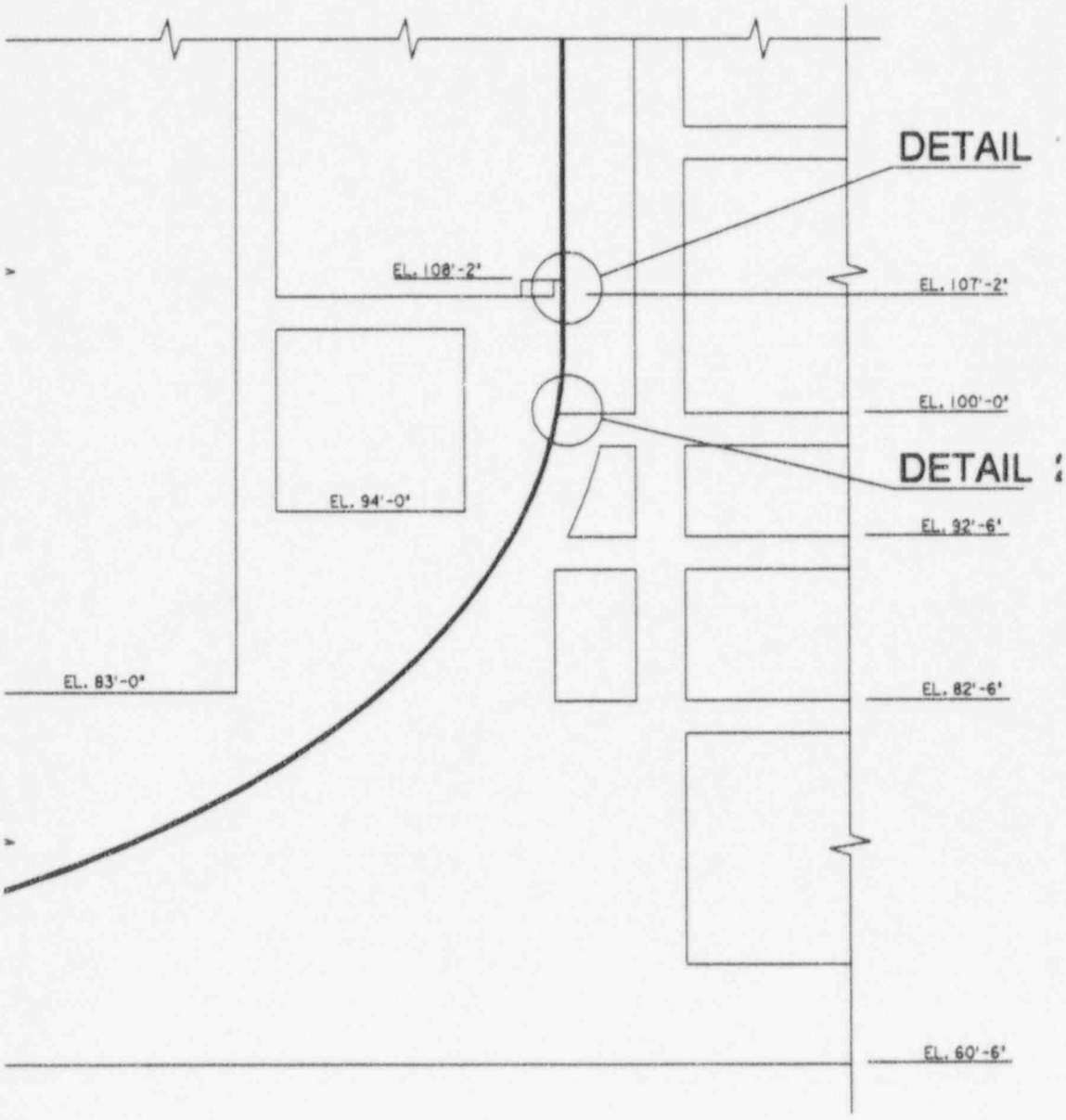

Figure 3.8.2-8 (Sheet 1 of 2)

Location of Containment Seal

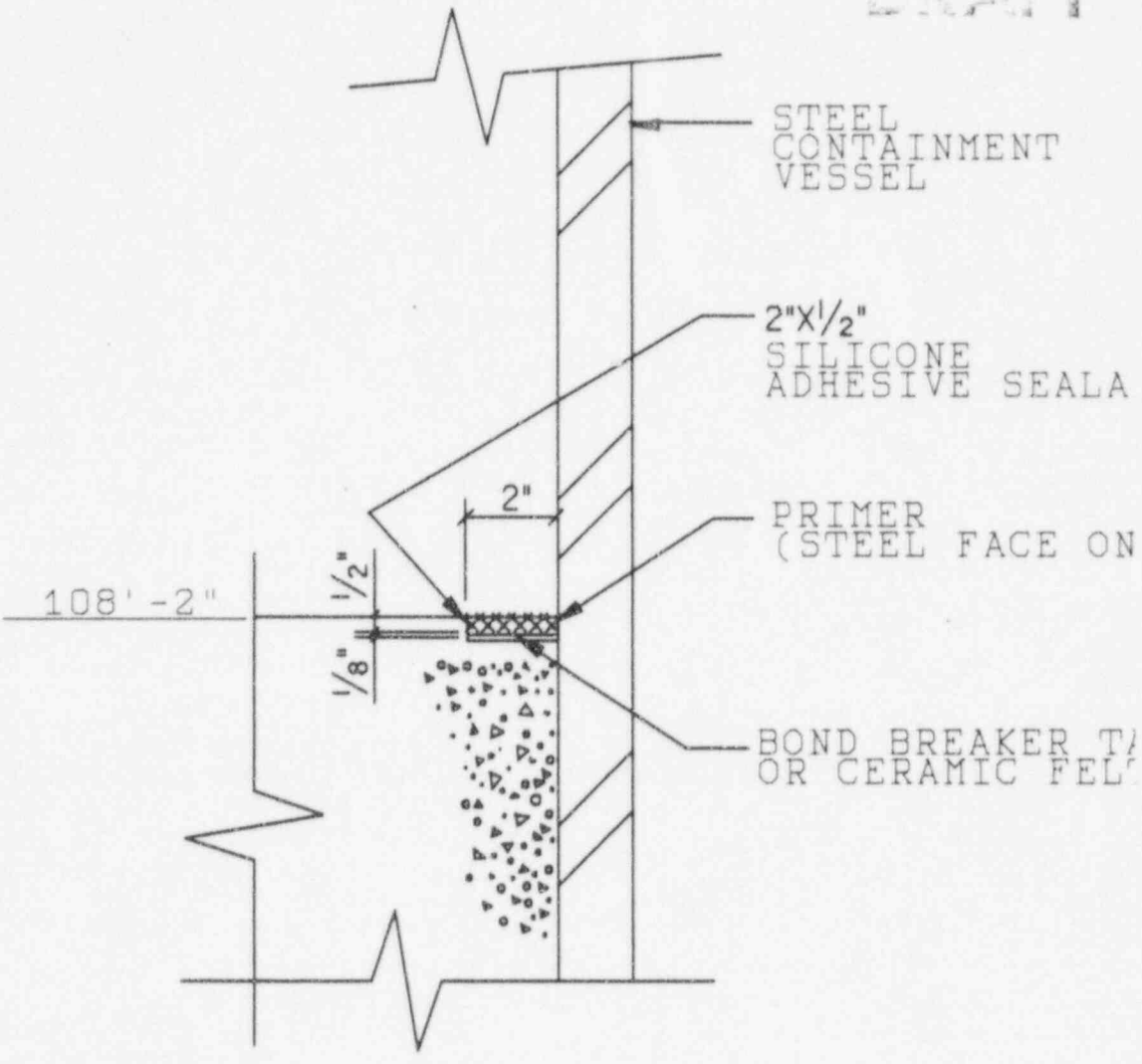

DETAIL 1

(DETAIL 2 SIMILAR)

Figure 3.8.2-8 (Sheet 2 of 2)

Seal Sections and Details

CHAPTER 42

CONDITIONAL CONTAINMENT FAILURE PROBABILITY DISTRIBUTION

42.1 Introduction

The probability distribution for containment failure due to internal pressurization of the containment has been developed for the AP600 containment vessel.

The AP600 containment and its structural properties are described in subsection 3.8.2 of the *AP600 Standard Safety Analysis Report* (SSAR). The limiting containment failure modes that have been identified include:

- General yielding of the cylindrical shell
- Buckling of the ellipsoidal head
- Buckling of the 22-ft. equipment hatch
- Buckling of the 16-ft. equipment hatch
- Yielding of the personnel airlock

Other containment failure modes are examined, as discussed in subsection 3.8.2 of the SSAR. Other failure modes, such as general yielding of the ellipsoidal head and failure of the piping penetrations, are not considered to be independent containment failure modes. Rather, these other failure modes are bounded by the failure criteria for the limiting failure identified above. Failures of the mechanical penetration bellows, and leakage of the equipment hatches due to ovalization, do not occur prior to general yielding of the cylinder. Failures of the electrical penetration assemblies do not occur prior to general yielding of the cylinder for temperatures equal to or less than 400°F.

Each of the limiting failure modes is examined to determine the best estimate of the failure pressure. In addition, the random and subjective uncertainties associated with each of the failure modes are identified. These failure characteristics are then used to develop a probabilistic model to predict the containment failure due to internal static pressurization. The details of the model development and the results of the analysis are presented in the following sections.

42.2 Probabilistic Model

To define the probability of a containment failure due to internal pressurization, it is necessary to select a statistical distribution with the correct properties. The engineering justification for a particular probability density function is made based on the gathering and evaluation of relevant information that can serve to characterize the nature of the random data and physical processes that lead to the random data. The nature of the random data, and in particular any limits or bounds on the data, are as important as the predicted means and variances from statistical analysis of the data. Thus, specific limits in the data and characteristics, such as

skewness, are utilized to specify the probability density function. Five potential probability distributions are considered: the Gaussian, the Gamma, the Gumbel, the lognormal, and the Weibull.

Based on a review of the characteristics of the five potential probability distributions, it was determined that both the Weibull and the lognormal distributions would be suitable to describe the containment failure probabilities. An additional review of the containment failure probability distributions reported in a number of the Individual Plant Examinations submitted to the Nuclear Regulatory Commission (in response to the Commission's Generic Letter 88-20) indicates that the lognormal distribution is the most commonly used distribution form for predicting containment failure from internal pressurization. Therefore, the lognormal distribution is selected to construct the conditional containment failure probability distribution.

42.3 Containment Failure Characteristics

The characteristic parameters for containment failure due to internal pressurization are derived from detailed analyses of the containment vessel, supplemented by applicable test data for certain design features of the containment, as described in subsection 3.8.2 of the SSAR. For the construction of the conditional containment failure probability distribution, the required characteristic parameters are the mean failure pressure and the statistical variance that represent the uncertainty associated with the mean value.

42.3.1 Mean Values for Containment Failure

The development of the conditional containment failure probability distribution requires the specification of the mean value for containment failure for each of the possible containment failure modes. Subsection 3.8.2 of the SSAR provides values for the ultimate containment pressure capability at 100°F and 400°F. These failure pressures are based on code specified minimum material properties. To obtain the mean and median values for the probability distribution, the failure pressures of subsection 3.8.2 of the SSAR are adjusted to account for the expected material properties and this adjusted best estimate failure pressure is considered as the median value of the lognormal distribution.

The containment vessel is designed using SA537, Class 2 material. This has a specified minimum yield of 60 ksi and minimum ultimate of 80 ksi. Test data for materials meeting SA537 or having similar chemical properties was reviewed from two United States and two Japanese steel suppliers. Some of the data was from tests of steel procured to SA537, Class 2, while the remaining data was identified by the steel supplier as having similar chemistry to SA537, Class 2 and being representative of SA537, Class 2. In a sample of 122 tests for thicknesses equaling or exceeding 1.50 inches and less than 1.75 inches, the actual yield had a mean value of 69.1 ksi with a standard deviation of 3.3 ksi, giving a mean yield value equal to 1.15 times the specified minimum yield with a coefficient of variation of 0.048. Test data for 389 tests for thicknesses from 0.31" to 3.16" showed a mean yield value of 71.7 ksi with a standard deviation of 5.7 ksi, giving a mean yield value equal to 1.19 times the specified minimum yield with a coefficient of variation of 0.079.

Reference 42-1 confirms that the actual yield strength of containment construction material can typically be expected to be 9 to 22 percent higher than the specified minimum material strength with coefficients of variation of 6 to 13% (the lower yield strengths reported are not appplicable to containment material; the ABS steel is procured to an ABS specification and not to ASTM; the static yield stress is a little lower than ASTM test yield). Since the mean containment strength is used to construct a probability distribution that includes random uncertainties in material properties as well as subjective uncertainties in modelling of the containment strength, it is appropriate to use the expected, as-built containment strength (i.e., the 15 percent increase over the nominal value) for the mean value of the distribution. However, since as-built information is not available for the AP600, the fragility is conservatively calculated using only a 10% increase above the specified yield and this value is used as the median value of the lognormal distribution.

The containment internal pressure value used for the median value of the containment failure probability distribution is the expected failure pressure, evaluated at 400°F. A review of the severe accident sequences in which the containment internal pressure approaches the failure pressure of the containment (including the decomposition event trees in Section 43 of the AP600 Level 2 PRA) leads to the conclusion that the containment shell is likely to be at the containment saturation temperature (for the internal containment pressure) for most severe accident sequences. With the passive containment cooling provided by the containment design, the highest likelihood of containment failure due to overpressurization is due to extreme cases of severe accident phenomena (e.g., hydrogen burns and noncoolable ex-vessel core debris). As described in Section 34, the temperature of the containment vessel steel does not significantly exceed the design temperature of 280°F. Therefore, the use of a uniform containment shell temperature of 400°F for evaluation of the containment material properties is bounding for the prediction of the conditional containment failure probability distribution.

The values used to construct the conditional containment failure probability distribution are identified in the next section.

42.3.2 Uncertainties in Containment Failure

The uncertainties identified and examined include both random uncertainties and subjective uncertainties. The broad categories of uncertainties considered are:

Geometric Properties: This category of uncertainty is principally concerned with the variations between the as-built containment vessel and the design utilized in the analysis. Some of these variations include containment dimensions, placement of stiffeners, and thickness of the steel plates used to make up the containment vessel. Also included in this category are construction practices such as the strength of weldments, etc. It has been reported [Reference 42-1] that the overall uncertainty in the containment strength is generally insensitive to variations in geometric properties, except for buckling mode of failure.

Structural Analysis: The uncertainties in the overall containment strength can be sensitive to uncertainties in assumptions and models used in the structural analysis of the ultimate strength of the containment structure. Some of the sources of uncertainty include: the definition of containment failure used in the analysis, the simplified geometric model used in the analysis, the analysis method, the analysis focus of failure locations and modes, the yield criterion for biaxial stresses, the rate of loading, the effect of non-uniform geometries, the effect of local temperature and the interpretation of test results to construct the analytical model. These uncertainties are subjectively evaluated since no complete investigation of these uncertainties is available. Reference 42-1 provides several estimates of the actual-to-predicted results, which vary according to the failure mode assumed in the analysis, the person doing the evaluation, and the method of analysis. The range suggested by these values is a mean value for the actual-to-predicted results tending to unity and a standard deviation in the range between 0.08 and 0.24. Reference 42-2 suggests that a value of 0.12 be used in constructing the probability distribution for the ultimate strength of the containment.

Material Properties: Uncertainties in material properties can be important in estimating the overall containment failure uncertainty. The total uncertainties in materials consider the estimation of statistical properties from a small sample (e.g., is the calculated mean the real mean) and assumptions on uniformity of properties. There is a wide range of application of material properties to estimate uncertainties and, except for the buckling mode of failure, most analyses neglect all uncertainties except the random, measurable variations in material properties. Reference 42-1 provides several estimates of the uncertainty in material properties that show a coefficient of variation in the range of 0.044 to 0.11 for conditions that may be applicable to the passive containment shell. Reference 42-2 recommends that a coefficient of variation between 0.06 and 0.08 be used to define the random variance in material properties for the containment shell. Finally, based on sampling of test results of material similar to that specified for the AP600 containment shell as described in subsection 42.3.1, the coefficient of variation was found to be 0.048.

Gross Errors: Gross errors in construction and / or design are not quantifiable since they lead to catastrophic results that are not predictable by reliability methods.

The values used to construct the conditional containment failure probability distribution are identified in the next section.

42.4 Containment Failure Predictions

42.4.1 Containment Cylindrical Shell

The response of the cylindrical portion of the containment vessel to internal pressurization has been analyzed, and the results reported in Table 3.8.2-2 of the SSAR. The best estimate of the pressure at which failure would occur is 120 psig, based on specified material properties at a uniform containment wall temperature of 400°F. This was adjusted to 132 psig to account for the expected actual material properties.

A coefficient of variation of 0.06 is used to represent the random uncertainty in material properties, consistent with the variability reported in subsection 42.3.1 for the sample of 122 tests of similar steel and with References 42-1 and 42-2. For the subjective uncertainty associated with modelling of the ultimate containment failure pressure, a coefficient of variation of 0.10 is used. This value is derived from Reference 42-1 (Table 5) for the analysis error (in-place / analytical result). It is the average of the coefficients of variation suggested for analyses based on limit analyses and axisymmetric finite element models. The predicted failure is based on the occurrence of large radial deflections of the shell and was estimated from both axisymmetric finite element analyses and hand calculations. The mean and coefficient of variation are supported by testing of scale model containment vessels, such as Reference 42-3 where gross yielding occurred within a few percent of the predicted pressure.

42.4.2 Ellipsoidal Upper Head

The response of the ellipsoidal upper head of the containment vessel to internal pressurization has been analyzed, and the results are reported in subsection 3.8.2 and Table 3.8.2-2 of the SSAR. Failure is predicted to occur either in the knuckle region or at the crown and may be initiated by buckling in the knuckle region. Failures due to tensile stresses (plastic collapse) are bounded by the variations considered for yield of the cylindrical shell. Only the buckling failure mode at the knuckle region can be considered to be an independent failure mode that must be separately considered in determining the conditional containment failure probability distribution.

The best-estimate internal pressure at which the ellipsoidal head of the containment vessel would fail due to post-yield buckling in the knuckle region is 145 psig, using minimum specified yield strength of the containment materials at 400°F. Since this buckling is associated with yield in the knuckle region, the capacity was adjusted to account for actual material properties by the ratio of actual to minimum yield to give a predicted pressure of 160 psig.

A coefficient of variation of 0.06 is used to represent the random uncertainty in material properties, consistent with the variability reported in subsection 42.3.1 for the sample of 122 tests of similar steel and with References 42-1 and 42-2. For the subjective uncertainty associated with modelling of the ultimate containment failure pressure, a coefficient of variation of 0.14 is used. This value is consistent with References 42-1 and 42-2 for the buckling mode of containment failure. It allows for uncertainties including those due to geometric properties (as-built condition) and residual stress.

42.4.3 Equipment Hatches

The response of the 22-ft. and 16-ft. diameter equipment hatches to internal pressurization has been analyzed, and the results are reported in subsection 3.8.2 of the SSAR. The containment internal pressure acts on the concave face of the dished head and the hatch covers are in compression under containment internal pressure loads. The predicted failure mode is elastic

buckling of the hatch covers. The best estimate of the pressure at which failure would occur for the 16-ft. equipment hatch is 226 psig at a uniform containment wall temperature of 400°F, based on 150 percent of the critical buckling pressure as indicated by a review of test data for buckling of spherical caps. The matching value for the 22-ft. hatch is 276 psig.

A coefficient of variation of 0.06 is used to represent the random uncertainty in material properties, consistent with the variability reported in subsection 42.3.1 for the sample of 122 tests of similar steel and with References 42-1 and 42-2. For the subjective uncertainty associated with modelling of the ultimate containment failure pressure, a coefficient of variation of 0.14 is used. This value is consistent with References 42-1 and 42-2 for buckling failures. It allows for uncertainties including those due to geometric properties (as-built condition) and residual stress.

42.4.4 Personnel Airlock

The response of the personnel airlock to internal pressurization has also been analyzed, and the results are reported in subsection 3.8.2 of the SSAR. The estimated pressure at which failure would occur is in excess of 300 psig, based on test results. Since the mean failure pressure is far above the mean failure estimates for the other containment failure modes, no further analysis of the personnel airlock is performed. Since its expected contribution to the overall containment failure probability distribution is negligible, it is not included further in the development of the conditional containment failure probability distribution.

42.5 Overall Failure Distribution

LATER

42.6 Summary and Conclusions

The cumulative containment failure probability distribution has been developed, using lognormal distribution, which is based on best-estimate predictions of containment strength and accounts for random uncertainties in material properties and subjective modelling uncertainties. Based on this model, the median internal pressure at which the AP600 containment vessel is predicted to fail is (later) psig. This is the best-estimate or expected containment failure pressure. This value is comparable to, or slightly higher than, the expected containment failure probability for other conventional pressurized water reactor (PWR) plants using pre-stressed or post-tensioned concrete containment structures.

The 5th and 95th percentile failure probabilities are (later) psig and (later) psig, respectively. The cutoff for consideration of containment failure due to internal pressurization during a severe accident is defined as the pressure at which the containment failure probability is less than 10^{-4}. Below this point the failure probability is so low that, when combined with the small core damage frequency numbers, the overall probability of a core damage accident resulting in containment failure is in the 10^{-10} range. This is generally considered to be a

negligible calculated number. From the lognormal distribution, the containment pressure corresponding to a 10^{-4} probability of failure is (later) psig.

42.7 References

42-1 "Reliability of Containments Under Overpressure," L. Greimann and F. Fanous, *Pressure Vessel and Piping Technology*, 1985, pp. 835 - 856.

42-2 "Reliability of Steel Containment Strength," L. Greimann, et. al., NUREG/CR-2442, June 1988.

42-3 "Comparisons of Analytical and Experimental Results from Pressurization of a 1:8 - Scale Steel Containment Model," Clauss, D.B. and Horschell, D.S., Proceedings 8th Intl. Conf. on SMiRT, Aug. 19 - 23, 1985

Table 42-1

PARAMETERS USED IN THE CONSTRUCTION OF THE AP600 CONTAINMENT FAILURE PROBABILITY DISTRIBUTION

Failure Location	Failure Mode	Median Failure Pressure[1] (psig)	Coefficient of variation	
			Material	Modelling
Cylindrical Shell	Membrane Yield	132	0.06	0.10
Ellipsoidal Head	Buckling	160	0.06	0.14
22-Ft. Equipment Hatch	Buckling	276	0.06	0.14
16-Ft. Equipment Hatch	Buckling	226	0.06	0.14
Personnel Hatch		300	0.06	0.14

[1] All median failure pressures are those specified at 400 °F

Table 42-2

CUMULATIVE CONTAINMENT FAILURE PROBABILITY

Containment Pressure (psig)	Probability of Containment Failure				
	Cylinder	Head	22-ft. Hatch	16-ft. Hatch	Total
	LATER				

AP600 Containment CCFP Calculations

Request for Additional Information, dated 9/14/95

Question # 1

In Chapter 42 of PRA SSAR, Rev. 4, the mean failure pressure is mentioned for each failure mode. As stated in DSER, the staff recommended the best estimate pressure be median for containment CCFP calculation. (If lognormal distribution is used, the mean is median times $\exp(\beta^2/2)$ where β is logarithmic standard deviation.) For the failure pressure estimates, the staff is not in a position to accept the 32% increase using both von Mises criterion and mean yield strength of SA537 Class 2 material. See Open Items 3.8.2.4-19 and 19 3.6.2-3.

- A comparison between experimental and theoretical yield stresses in Engineering Design, Faupel, J.H., pp. 249-258, John Wiley & Sons, 1964 shows that the von Mises yield criterion does not always give a 15 percent higher yield stress than that obtained from the maximum shear stress criterion,

- The material test data uses only 122 specimen and they are neither exactly the same as the SA 537, Class 2 material nor as-built material,

- In "Comparisons of Analytical and Experimental Results from Pressurization of a 1:8 - Scale Steel Containment Model," Clauss, D.B. and Horschell, D.S., Proceedings 8th Intl. Conf. on SMiRT, Aug. 19 - 23, 1985, and NUREG/CR-4209, the measured yield pressure was reported 15% less than that predicted yield pressure ($r = 84"$, $t = 0.197"$, $\sigma_y = 57.1$ ksi, $P = \sigma_y t/r = 134$ psig) using MARC FEM code with large displacement, nonlinear material property obtained from standard uniaxial tensile tests (test coupons were machined from remnants and cutouts for the penetrations), and von Mises yield criterion due to (1) strain rate effects (5% reduction), (2) Bauschinger effect (5 to 10% reduction) referring to the phenomenon whereby the yield stress in tension or compression is reduced if the material has been previously yielded in the opposite sense (when the plates comprising the cylinder were rolled into the cylindrical shape, the internal surface underwent compressive yielding and internal pressurization results in tensile yielding in the cylinder), and (3) difficulties in applying uniaxial data to multiaxial strain states,

- From an American Iron and Steel Institute (AISI) survey of test results for thousands of individual product samples, it has been found that strength levels vary as much as 20 percent from the certified material test reports (CMTR) test values. It has been the staff's position that minimum specified strength values (e.g., ASME Code minimum strength values) should be used as the basis for allowable stresses as described in the letter from G. Bagchi and C. Cheng to J. Stolz, Subject: Review of Oyster Creek Drywell Containment Structural Integrity, dated June 14, 1990.

Response

PRA Chapter 42 will be revised to use the lognormal distribution with the best estimate pressure considered as median for the containment CCFP calculation. The best estimate pressure for the cylinder will be based on the von Mises yield criterion and median actual material properties 10% above the ASME specified yield. The examples quoted in the RAI are discussed below. These examples are considered in the selection of the material and modelling uncertainty coefficients of variation.

- The von Mises yield criterion is a theoretical criterion that does give a 15 percent higher yield stress than that obtained from the maximum shear stress criterion for the stresses due to pressure in a cylindrical vessel (longitudinal stress equal to one half hoop stress). Test data shown in the reference indicate "slightly better agreement with the distortion energy theory (von Mises) than with the shear theory". In the tension-tension interaction portion the test data is between the shear theory (1.00 factor) and the distortion energy theory (elliptical interaction curve with maximum equal to $2/\sqrt{3} = 1.155$. Most text books recommend the distortion energy theory and this is the basis included in the BOSOR-5 analyses performed for the AP600.

  The uncertainty in yield criterion is a part of the modelling uncertainty.

- The material test data quoted in the SSAR refers to 122 tests where the plate thickness was between 1.50" and 1.74" and gave a mean value of 69,100 psi with a standard deviation of 3,300 psi. This was quoted since it was most representative of the 1.625" thickness for the AP600. Test data for 389 tests for thicknesses from 0.31" to 3.16" showed a mean value of 71,700 psi with a standard deviation of 5,700 psi. This test data came from two United States and two Japanese steel suppliers. Some of the data is from tests of steel procured to SA537, Class2, while the remaining data was identified by the steel supplier as having similar chemistry to SA537, Class 2 and being representative of SA537, Class 2.

  The results for the 122 tests give a mean value equal to 1.15 times the specified yield with a coefficient of variation of 0.048. This is similar to that for A 516 grade 50 material (mean = 1.19 times the specified yield, COV = 0.08) quoted in Table 1 of "Reliability of Containments under Overpressure" (PRA Chapter 42, reference 42-1)

- NUREG/CR-4209 reports a predicted membrane yield pressure of 180 psig for the 1:8 scale model. This prediction is described in NUREG/CR-4137, where it is described as general yielding of the cylinder (page 15). The prediction is based on an axisymmetric finite element analysis described in Section 6.1 of NUREG/CR-4137, where the ring stiffeners and shell are modelled. Typical analysis results of the ring stiffened cylinder are shown in Figures 8 and 9. The effect of the rings is to restrain a portion of the shell while the cylinder midway between ring stiffeners expands further; the rings therefore increase the pressure capacity corresponding to gross yielding of the cylinder as a whole. As the pressure is increased, local yield initiates and loads are shared by the stiffener rings. General membrane yield does not occur until both the shell and the rings reach yield. This is best observed from radial displacement plots from which yield pressure corresponds to the pressure at which the radial displacement rapidly increases. Unfortunately deflection data for the test was not complete and only strain data is available.

  The yield capacity of 134 psig calculated in the question uses the shear yield criterion and average thickness for an unstiffened cylinder. The capacity may also be estimated from the uniaxial yield stress (57,100 psi), the radius (84 inches), the nominal thickness (0.1875") and the stiffener rings (2.75" x 0.1875", 15" spacing). The shell is in biaxial tension and yield is calculated using the von Mises criterion. The ring is in uniaxial tension.

  Unstiffened cylinder: $p_{us} = \sigma_y / R \times 2/\sqrt{3} \times t$
  $= 57100 / 84.09 \times 1.155 \times 0.1875$
  $= 147$ psig

Stiffened cylinder: $p_s = \sigma_y / R \times (2/\sqrt{3} \times t + A_s)$
$= 57100 / 84.09 \times (1.155 \times 0.1875 + 2.75 \times 0.1875 / 15)$
$= 170$ psig

NUREG 4209 reports an average plate thickness of 0.197". This would increase the above capacities to 155 psig and 179 psig. The stiffeners are far enough apart that the shell mid way between ring stiffeners acts elastically as an unstiffened cylinder. Thus, the expected behavior would be that the cylinder near the midpoint between ring stiffeners will yield when the pressure reaches 155 psig and additional load is carried by the shell bending between the ring stiffeners. This leads to yield at the ring stiffener due to combined hoop and longitudinal strains, and thereby reaches the general yield pressure at 179 psig. This is consistent with the predicted capacity of 180 psig given in NUREG/CR-4209. Note that yield would be predicted to start at a pressure of 155 psig which is equal to the pressure at which the NUREG reports that it started.

NUREG/CR-4209 reports that membrane yielding for most of the cylinder occurred between 155 and 171 psig. The lower end of this range is believed to be yield of the cylinder between stiffeners and does not represent general membrane yielding of the stiffened cylinder. Yielding of one ring stiffener is shown in Figure 10 at a pressure of about 163 psig. General membrane yielding (shell / ring combined) leading to large radial deflections does not occur until all of the cylinder reaches membrane yield and can be assumed to occur between the 163 psig for the ring in Figure 10 and the 171 psig magnitude reported as the upper end of the yield range (the third paragraph of Section 9 of NUREG / CR 4216 also states that, up to the pressure of 170 psig, a single yield plateau was not observed). This is 5 - 10% below the predicted capacity for the smeared stiffeners.

The difference of 5 - 10% in the test and analytical results for gross yield of the 1:8 model is reported in the referenced NUREGs as being due to a combination of the strain rate and the Bauschinger effect. It could also be due to inaccuracies in the von Mises criterion as discussed in the first bullet. The difference of 5 - 10% in the test results is small and is accounted for in the AP600 fragility estimates in the coefficient of variations assigned to materials and modelling uncertainties.

- Steel yield test data is summarized in the paper "Reliability of Containments under Overpressure" (PRA Chapter 42, reference 42-1). The steel for the AP600 will be procured to ASME requirements which should result in better quality than the range of data reported in the AISI survey. Specific examples are described in previous paragraphs.

  The staff's position that minimum specified strength values (e.g., ASME Code minimum strength values) should be used as the basis for allowable stresses is the basis for allowable stresses for design loads and not to the "best estimate failure analysis". Other fragility evaluations have used best estimate yield properties based on 10% above the specified values. Westinghouse will also use this assumption in updating the fragility calculation.

Question # 2

In Section 42.2, is lognormal distribution applicable for the 16-ft and 25-ft equipment hatches? Due to their convexity, these are under compression when subjected to containment internal pressure as mentioned, further justification is necessary for these equipment hatches.

Response

The 16-ft and 25-ft equipment hatch covers are arranged such that, due to their convexity, they are under compression when subjected to containment internal pressure. The internal pressure is defined for the whole containment vessel; however, the hatch covers are designed using the ASME rules for external pressure loading (NE-3133 and Code Case N-284). In sections of the SSAR and PRA report discussing equipment hatch pressure capacity, a statement has been added that the internal pressure acts on the convex face and the cover is in compression.

Distribution is primarily influenced by imperfection. Measured imperfection must be less than ASME specified limit. Use of lognormal distribution is considered appropriate, similar to its use for material yield which must also exceed a minimum ASME specification.

Question # 3

In Section 42.3.1, Ref. 42-1 did not provide data showing that the actual yield strength of containment construction materials could be 12 to 22 percent higher than the specified minimum material strength. The range is 2.5 to 22 percent in Table 1. Also, there is no data for SA537, Class 2 material in Ref. 42-1.

Response

Section 42.3.1 has been revised. The reference includes two sets of relatively low data. One set is ABS steel which is not covered by an ASTM specification, and may not have a specified yield. The other set is static yield values which are at a lower strain rate than the ASTM test specification.

Question # 4

In Section 42.4, provide uncertainties for geometric properties (as-built condition) and residual stress for buckling of knuckle area and equipment hatch covers. Imperfection for internal pressure is insensitive, however, for external pressure, it should be significant. (from N-284, capacity reduction factor is considered for imperfection and plasticity of nonlinear material properties.)

Response

Section 42 has been revised to state that the COV includes consideration of these uncertainties.

Question # 5

In Section 42.4.1, how is the COV of 0.1 derived from Ref. 42-1? The Table 4 of Ref. 42-1 shows only the thickness of 1-1/4" thickness (mean = 1.277", σ = 0.012", COV = 0.01) and it assumes normal distribution, not lognormal distribution. Also, this COV of 0.01 represents the uncertainty for geometric properties, not modeling error. The Ref. 42-1 shows the modeling error COV of 0.144 from $(0.12^2 + 0.08^2)^{1/2}$ in Table 7. The COV for all practical purposes of modeling error which should include nonsymmetric features such as penetrations and other reinforced openings, longitudinal stringers, etc. as well as circumferential variations in thickness, ring and stringer sizes, amount of reinforcing steel, and

shell imperfection is 0.12 (Ref. 42-2). The staff believes that the use of the COV of 0.1 results in unconservative CCFP calculation. See Open Items 3.8.2.4-21 and 19.2.6.3-1.

Response

The value of 0.10 is derived from Reference 42-1 (Table 5) for the analysis error (in-place / analytical result). It is the average of the coefficients of variation suggested for analyses based on limit analyses and axisymmetric finite element models. The predicted failure is based on the occurrence of large radial deflections of the shell and was estimated from both axisymmetric finite element analyses and hand calculations. The mean and coefficient of variation are supported by testing of scale model containment vessels, such as Reference 42-3 where gross yielding occurred within a few percent of the predicted pressure.

Question # 6

In Section 42.4.2, provide mean (median) failure pressures with modeling and material uncertainties for crown yield, knuckle area yield, and knuckle area buckling. Imperfection uncertainty is insignificant due to internal pressure buckling (See N-284).

How is 192 psig derived in knuckle area? Is it 146*1.15*1.15?

How is 144 psig derived for ellipsoidal head buckling failure mode in Table 42-1? It is not given in SSAR. Is it derived from 174 x 138/166?

For the ellipsoidal head, there are two possible failure modes, i.e., asymmetric buckling (P_{cr}) and plastic collapse (P_c). Therefore, the plastic collapse pressure information should be considered in SSAR.

Response

SSAR and Section 42 have been revised to clarify that failure mode of the top head is represented by knuckle buckling. The other failure modes, including plastic collapse, are bounded by the case for knuckle buckling.

The value of 192 psi in paragraph 42.4.2 should have been 174 psi. The value of 144 in Table 42-1 should have been 163. Both have been revised due the change in mean value of the actual material yield (see RAI # 1).

Question # 7

In Section 42.4.3, Westinghouse increases 50% critical pressure for the best estimate failure pressure based on N-284 curve which was derived from lower bound of tests. However, there was only one test performed for AP600 containment configuration (M_i = 14.5). Therefore, it is believed that 50% curve from tests might be appropriate use for AP600 containment. (N-284 does not provide 50% and upper bound curves.) Are test data in N-284 applicable to AP600? They seem to be stiffened spheres.
Also, in NUREG/CR-4209 and -4137, equipment hatch has critical pressure of 3,000 psig and the predicted response of the cover and tensioning ring was elastic up to 360 psig. In this case, only up to 12% of critical pressure is elastic. After that, equipment hatch cover will experience plastic deformation.

Therefore, Westinghouse's claim that the failure pressure is 150% of critical pressure is questionable. See Open Items 3.8.2.4-26 and 19.2.6.3-6.

Equipments hatches are subjected to external pressure, not internal pressure.

Response

The test data on spherical caps was included in the response to RAI 220.32. This data is representative for a large range of "M" values. The mean value of the data is greater than 1.50 times the Code Case N-284 criteria. The value of 1.50 was used conservatively in the AP600 fragility evaluation. For the AP600, buckling of the hatch covers is elastic.

Question # 8

In Section 42.5, provide the sample CCFP calculations for head at 100 psig. You have constructed the containment failure probability distribution for a particular failure mode by first developing the failure distribution assuming only random error and then developing another distribution assuming only subjective error. The staff believes this method may not be conservative in comparison with the combination of random and subjective errors ($\beta_c^2 = \beta_{material}^2 + \beta_{modelling}^2$) in the left tail region.

Response

Westinghouse will update the fragility analysis using an SRSS combination of random and subjective errors.

Question # 9

In Section 42.6, what is the definition of mean internal pressure? Should it be median pressure? See Open Items 3.8.2.4-27 and 19.2.6.3-7.

Response

Agreed. Revise to median internal pressure.

Question # 10

In Table 42-1, does "Structural" under COV heading imply "Material"?

Response

Agreed. Revise "structural" to "material".

Question # 11

In Table 42-2, 50% failure pressure for head seems to be around 156 psig. Where does this pressure come from?

Response

Table 42-2 will be revised. Revised methodology outlined in responses to other RAIs should resolve this issue.

Question # 12

In Section 42.4, coefficient of variation, not coefficient of variance, should be used.

Response

Agreed. Section 42 has been revised.

Question # 13

In SSAR Subsection 3.8.2.4.2.5, EPAs to be used will be one of those tested by Sandia in NUREG/CR-5334:

D.G. O'Brien: 182.8°C (361°F) and 1,068.7 kPa (155 psia) for 10 days,
Westinghouse: 204.4°C (400°F) and 517.1 kPa (75 psia) for 10 days,
Conax: 371.1°C (700°F) and 930.8 kPa (135 psia) for 10 days

If Westinghouse EPAs will be used for AP600, they do not satisfy ASME Service Level C limits (90 psig at 400°F). Also, in fragility curve, the dominant failure mode is cylindrical shell with 138 psig at 400°F. Therefore, if they are used, they control the whole design both in deterministic and probabilistic. The fragility curve for EPAs should be provided.

Response

SSAR and PRA report have been revised. Based on latest severe accident analyses documented in PRA Section 34, the shell temperature does not exceed design temperature of 280°F. Hence, the qualification for Design Basis plus Sandia tests provides basis that temperature does not affect capacity. Structural evaluation of plate capacity is then sufficient.

Question # 14

In Section 42.4, if the bellow capacity is 90 psig at 400°F, what is probability of failure beyond this pressure? Westinghouse should provide the mean (or median) failure pressure, and uncertainties of geometric properties, modeling, and material for complete CCFP calculations.

Response

PRA report now states that bellows fragility is included in cylinder yield fragility.

Question # 15

In Section 3.8.2.4.2.2, the maximum deflection at crown is 15.9" at 174 psig and corresponding strain is 2.5%. Therefore, radius is 15.9/0.025 = 636". Where does this radius come from? The radius, R_s, is 1,347.5".

Response

In Section 3.8.2.4.2.2, the reported strain is the effective (von Mises) strain. The circumferential and meridional strain at the crown are about one half of the effective strain or 1.25%. The radius of curvature at the crown, calculated based on equilibrium, is 1105" at the internal pressure of 174 psig. This is consistent with the radius of curvature at this pressure in the large displacement non-linear BOSOR-5 analysis.